

# 1 Tsunami damage to ports: Cataloguing damage to create fragility 2 functions from the 2011 Tohoku event

3  
4 Constance Ting Chua <sup>1,2</sup>, Adam D. Switzer <sup>1,2</sup>, Anawat Suppasri <sup>3</sup>, Linlin Li <sup>4</sup>, Kwanchai Pakoksung <sup>3</sup>,  
5 David Lallemand <sup>1,2</sup>, Susanna F. Jenkins <sup>1,2</sup>, Ingrid Charvet <sup>5</sup>, Terence Chua <sup>1</sup>, Amanda Cheong <sup>6</sup> and Nigel  
6 Winspear <sup>7</sup>

7  
8 <sup>1</sup> Asian School of the Environment, Nanyang Technological University, Singapore

9 <sup>2</sup> Earth Observatory of Singapore, Nanyang Technological University, Singapore

10 <sup>3</sup> International Research Institute of Disaster Science, Tohoku University, Sendai, Japan

11 <sup>4</sup> School of Earth Sciences and Engineering, Sun Yat-Sen University, Guangzhou, China

12 <sup>5</sup> Formerly Department of Statistical Science, University College London, London, United Kingdom

13 <sup>6</sup> JBA Risk Management Pte Ltd, Singapore

14 <sup>7</sup> Formerly SCOR Global P&C, Singapore

15

16 *Correspondence to:* Constance Chua (CCHUA020@e.ntu.edu.sg)

17 **Abstract.** Modern tsunami events have highlighted the vulnerability of port structures to these high-impact but infrequent  
18 occurrences. However, port planning rarely includes adaptation measures to address tsunami hazards. The 2011 Tohoku  
19 tsunami presented us with an opportunity to characterise the vulnerability of port industries to tsunami impacts. Here, we  
20 provide a spatial assessment and photographic interpretation of freely available data sources. Approximately 5,000 port  
21 structures were assessed for damage and stored in a database. Using the newly developed damage database, tsunami damage  
22 is quantified statistically for the first time, through the development of damage fragility functions for eight common port  
23 industries. In contrast to tsunami damage fragility functions produced for buildings from existing damage database, our  
24 fragility functions showed higher prediction accuracies (up to 75% accuracy). Pre-tsunami earthquake damage was also  
25 assessed in this study, and was found to influence overall damage assessment. The damage database and fragility functions for  
26 port industries can inform structural improvements and mitigation plans for ports against future events.

27

## 28 **1. Introduction**

29 Port assets are vulnerable to the physical damage caused by tsunamis and cascading effects such as extensive supply chain  
30 disruption. For example, transoceanic waves from the 2004 Indian Ocean tsunami resulted in heavy damage to maritime  
31 facilities across the Indian Ocean. On the west coast of Banda Aceh, Indonesia, all harbours and landing piers between Lhok  
32 Nga and Meulaboh were destroyed and unusable (Janssen, 2005) and across the Indian Ocean, heavy damage to maritime  
33 facilities reportedly resulted in the closure of Nagappattinam Port, India for weeks (Mahshwari et al., 2005). On the same note,  
34 the 2011 Tohoku (Great East Japan) tsunami caused damage to many ports along the Pacific coast in the Tohoku region. The  
35 affected ports suffered from a contraction in export and import values following the tsunami (March – May 2011) of 57.5%  
36 and 61.6% respectively, relative to the preceding 5-year average for the same period (Japan Maritime Centre, 2011). Total  
37 economic losses for tsunami damage to Japan’s marine vessels, ports and maritime facilities were approximated at US\$ 12  
38 billion (Muhari et al., 2015). A recent study speculated that earthquakes greater than Mw 8.5 from the Manila-trench could  
39 result in the loss of functions in up to five major ports including Kaohsiung and Hong Kong (Otake et al., 2019). Additionally,  
40 threats from future tsunami events are expected to be exacerbated by rising sea levels (Li et al., 2018), which imply greater  
41 risks for port assets located near tsunami sources.

42 With about 80% of global trade volume carried by sea, ports are critical nodes in international trade. Ports are also home to  
43 industrial clusters and critical facilities such as manufacturing firms and power plants due to the convenience they provide.  
44 With increased seaborne trade, globalisation of complex industrial processes and dependence on ports for economic  
45 development, port areas are only expected to develop further. However, port planning rarely accounts for adaptation to natural  
46 hazards and coastal protection structures are usually built to mitigate short-term hazard scenarios such as coastal flooding and  
47 wave damage (Lam and Lassa, 2017).

48 Tsunamis are high-impact events but infrequent occurrences, which makes their potential impacts to ports difficult to quantify.  
49 The expected increase in the exposure of port assets to coastal hazards, combined with our limited experience with tsunamis  
50 in modern ports, demonstrates a clear need to better understand how port structures might respond to tsunami impacts.

51 Structural damage resulting from tsunami impacts has generated considerable interest since the 2004 Indian Ocean tsunami  
52 (e.g. Nistor et al., 2010, Leelawat et al., 2016; Song et al., 2017; Suppasri et al., 2019). Structural damage is most commonly  
53 quantified in the form of tsunami damage fragility functions. First developed for tsunami events by Koshimura et al. (2009),  
54 tsunami fragility functions express the probability that a structure exceeds a prescribed damage threshold for a given tsunami  
55 flow characteristic or intensity measure. Pioneering work in the development of tsunami fragility functions has been largely  
56 focused on damage to residential and commercial buildings (e.g. Leone et al., 2011, Reese et al., 2011; Mas et al., 2012; Gokon  
57 et al., 2014). In recent years, the study of tsunami structural fragility has been extended to critical infrastructure such as roads  
58 and bridges (Akiyama et al., 2014; Shoji and Nakamura, 2017; Williams et al., 2020).

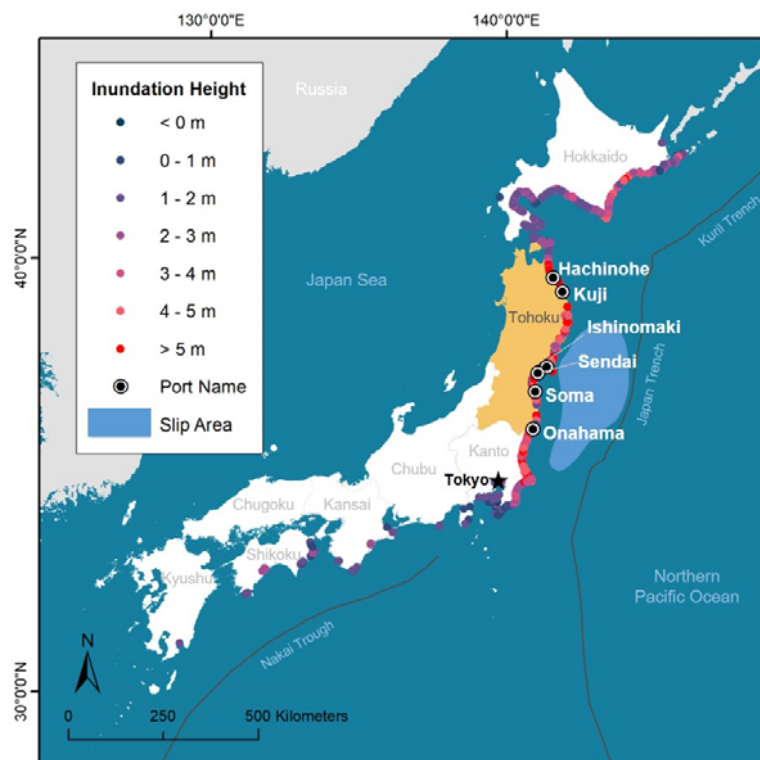
59 Despite recent efforts, our understanding of tsunami impacts on ports still falls short. The coverage of tsunami-induced damage  
60 on port structures in existing literature is by and large limited to qualitative assessments. To date most studies on tsunami

61 structural damage to ports are in the form of post-tsunami surveys, which document damage observations and describe the  
62 failure mechanisms of harbour elements such as breakwaters, quay walls and wharves (e.g. Meneses and Arduino, 2011; Fraser  
63 et al., 2012; Hazarika et al., 2013; Paulik et al., 2019; Benzair et al., 2020) and port facilities such as oil tanks, cranes and  
64 equipment (e.g. Scawthorn et al., 2016; Percher et al., 2013; Sugano et al., 2014). Some studies have attempted to reconstruct  
65 structural impacts to port facilities by evaluating design specifications of structures or examining specific tsunami behaviour  
66 such as bore impact linked to structural damage (e.g. Nayak et al., 2014; Kihara et al., 2015; Chen et al., 2016; Huang and  
67 Chen, 2020). Though recent studies attempted to quantify tsunami damage to port facilities, the focus of these standalone  
68 studies are specific to certain port industries, namely warehousing (Karafagka et al., 2018) and fishery industries (Imai et al.,  
69 2019), and therefore do not provide a comprehensive view of the damage sustained by different port industries. While  
70 necessary for the improvement of structural design, efforts so far are not adequate in quantifying tsunami damage statistically.  
71 This study serves as a starting point in characterising the vulnerability of port industries to tsunami impacts, through the  
72 assessment and quantification of structural response to tsunami inundation depths. The objective of this study is two-fold – (i)  
73 to develop a tsunami damage database for port structures impacted during the 2011 Tohoku tsunami, and based on the damage  
74 database, (ii) to construct tsunami damage fragility functions for port industries. The 2011 Tohoku tsunami presents a unique  
75 opportunity to study tsunami damage to port structures due to the extent and severity of damage, and the large ensemble of  
76 data collected post-tsunami (Table 1). The combination of densely recorded tsunami flow measurements, well-documented  
77 surveyed damage data and high-quality photographic evidence available offers an unparalleled resource for this research.  
78 In this paper, we develop the first tsunami damage database for port industries and their related structures. We also present the  
79 first sets of tsunami damage fragility models for common industries found in the port hinterland. We describe the data sources  
80 and methods to develop this damage database, and demonstrate in detail how the damage database addresses limitations found  
81 in past studies. Fragility functions are constructed by reviewing and employing best practices in the field. Unique to this work,  
82 we also evaluated the robustness of tsunami fragility functions against the influence of pre-tsunami earthquake effects. We  
83 conclude by highlighting some key application opportunities of this dataset and providing recommendations for overcoming  
84 current limitations found in this study. This study provides a blueprint for translating post-event damage surveys into fragility  
85 functions, which can be used to forecast future tsunami-induced damage to ports.

## 86 **2. Study site**

87 The northeast coast of Japan, also known as the Tohoku region, was severely impacted by the Tohoku tsunami on 11 March  
88 2011 (Fig. 1). Port operations along the Pacific Coast in Tohoku and eastern Kanto regions were disrupted due to debris and  
89 severe damage to buildings, loading facilities, wharfs, fuel facilities and seawalls (Takano et al., 2012). Damage patterns varied  
90 along the Tohoku coastline. The Tohoku coastline is mainly coastal plains and ria coasts. Coastal plains are extensive areas of  
91 low-lying flat terrain, while ria coasts, formed by submergence of former river valleys, typically have limited flat terrain. Ria  
92 coasts are characterised by narrow funnel-shaped coastal inlets bounded by steep slopes such as mountains. In coastal plains,

93 damage severity transitioned gradually with distance inland, decreasing as inundation depths decrease with distance inland  
 94 (De Risi et al., 2017). In ria coasts, the spatial distribution of damage was uneven because flow characteristics i.e. velocity and  
 95 hydrodynamic force, which influence damage severity, varied significantly for different points at the same distance inland or  
 96 with similar inundation depths (Suppasri et al., 2013; De Risi et al., 2017). This was due to the differences in local topography  
 97 (Tsuji et al., 2014). Coastal topography influences tsunami behaviour on land, and therefore influences tsunami flow dynamics  
 98 and inundation characteristics (Suppasri et al., 2015). Previous studies have highlighted the importance of separating the two  
 99 types of coastlines when assessing tsunami damage (Suppasri et al., 2013; Tsuji et al., 2014; De Risi et al., 2017). This study  
 100 focuses on ports located in coastal plains, due to the (i) difficulty of accounting for complexity of flow processes in ria coasts  
 101 as well as (ii) significantly less port activity found in the narrow strips of ria coasts. Affected ports, namely Hachinohe, Kuji,  
 102 Ishinomaki, Sendai, Soma and Onahama, located in coastal plains were selected as study sites for our damage assessment (Fig.  
 103 1).  
 104

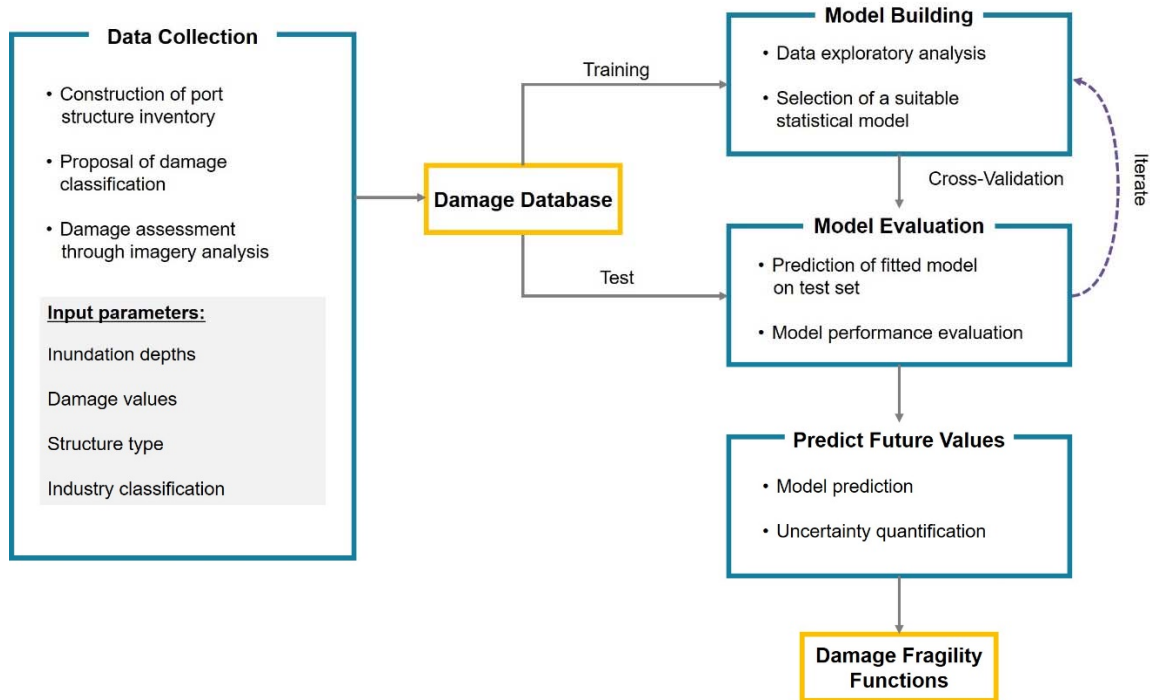


105  
 106 **Fig. 1.** Six of the affected ports (circled dots) were selected in this study due to similarities in their coastal morphologies –  
 107 they are located in coastal plains. Tsunami inundation heights were measured and collected by the Tohoku Tsunami Joint  
 108 Survey (TTJS, 2011) team. Inundation heights refer to the maximum height of tsunami inundation above the mean sea level  
 109 in Tokyo Bay (the Tokyo Peil datum). The generalized 2011 fault-rupture area (in light blue) was inferred from GPS data  
 110 adapted from Ozawa et al. (2011).

111 **3. Workflow and data sources**

112 A goal of this study was to produce tsunami damage fragility functions for industries commonly found in ports and their  
113 hinterlands, such as chemical and energy-related industries. The components required to derive fragility functions include the  
114 explanatory variable (hazard intensity measure), response variable (damage data) and a statistical linking model (Charvet et  
115 al., 2017). At present, a consolidated data source for tsunami damage to port structures has yet to exist. This data gap presents  
116 us with an opportunity to develop a damage database for port structures, and to use the damage data for the construction of  
117 fragility functions. We developed a framework (Fig. 2) for collecting and processing damage data within a database and using  
118 a machine learning workflow to evaluate those data and provide robust fragility functions; more details on our approaches are  
119 provided over the following subsections. We used freely available data where possible to illustrate how our methods can also  
120 be reproduced in other locations. A synopsis of the data used in this study and their sources are presented in Table 1.

121



122

123 **Fig. 2.** The framework of this study follows the approach of a machine learning workflow. A damage database for port  
124 structures is constructed through data collection and processing. The consolidated data is then randomly split into training and  
125 test sets for model building and evaluation. This process is usually iterated until a satisfactory model is selected for the  
126 development of fragility functions. This is usually the case where there are more than one model or parameter to choose from,  
127 whereas in our case, only inundation depth was considered as an explanatory variable.

128

129 **Table 1.** Data used in this study, their sources and the reference period from which data are taken.

<b>Data</b>	<b>Source</b>	<b>Data observation/ acquisition period</b>	<b>Citation</b>
Tsunami inundation depths	Ministry of Land, Infrastructure, Transportation and Tourism (MLIT)	Mar 2011 – Dec 2012	Ministry of Land, Infrastructure, Transportation and Tourism (2014)
Building database	Ministry of Land, Infrastructure, Transportation and Tourism (MLIT)	Mar 2011 – Dec 2012	Ministry of Land, Infrastructure, Transportation and Tourism (2014)
Port structure footprint for digitisation	GSI Interactive Web: Map/Aerial Photo Browsing Service;	-	Geospatial Information Authority of Japan (2013)
	Google Earth engine	Mar 2009 – Sep 2010	© Google Earth 2020
Aerial images for damage assessment	Google Earth engine;	Mar 2009 – Sep 2010 + Mar 2011 – May 2011 ++ Feb 2012 +++	© Google Earth 2020
	GSI Map: Aerial Photo of Affected Area	Mar 2011 – May 2011 ++ Apr 2012 +++	Geospatial Information Authority of Japan (2012a)
Oblique images for damage assessment	GSI Map: Oblique Photo of Affected Area	May 2011 ++	Geospatial Information Authority of Japan (2012b)
Street view images for damage assessment	Google Street View	Jul 2011 – Aug 2011 ++ Aug 2013 +++	© Google Street View 2020
Landuse (industry) classification	Google Maps	-	© Google Maps 2020

+Pre-tsunami, ++Immediate phase after tsunami and +++One to two years after tsunami (Intermediate phase) for damage assessment

131 **4. Data collection**

132 **4.1 Establishing a damage database**

133 The port structures referred to in this study collectively consist of a mixture of buildings and industry-related non-building  
134 structures (henceforth referred to as port infrastructure). Detailed building damage data have been collected by Ministry of  
135 Land, Infrastructure, Transportation and Tourism (MLIT, 2014) post-tsunami. However, the MLIT database predominantly  
136 consists of residential, commercial and some industrial buildings. Buildings within the port area are mostly missing from the  
137 database, and infrastructure such as silos, cranes and towers were not identified in the MLIT database.

138 To develop our own database of port structures, we extended the MLIT database, which already consisted of outlines of 3,057  
139 buildings. To build the new database, port structure outlines (n = 2,173) were digitised into a Geographic Information System  
140 (ArcMap 10.5) using building footprints from the Geospatial Information Authority of Japan Interactive Map platform (GSI,  
141 2013) as well as pre-tsunami aerial images from Google Earth Engine (Table 1). We identified 3,343 buildings and 1,887  
142 infrastructure (5,230 total). The database is stored in the form of a Geographic Information System (GIS) attribute table. For  
143 each structure, we collected information on

- 144 (1) the type of industry
- 145 (2) the name of port
- 146 (3) the name of company at the time of tsunami (where available)
- 147 (4) maximum inundation depth values
- 148 (5) assigned damage state and,
- 149 (6) structure type (building or infrastructure)

150 **4.2 Attributes of port structures and industry**

151 Unique to this work, damaged structures were classified according to their industry type (Table 2). As with the construction  
152 of any fragility function, a key assumption is that structures under the same taxonomy are likely to perform similarly when  
153 exposed to a given hazard intensity (Pitilakis et al., 2014). For that reason, the classification of structures determines the  
154 robustness of the fragility functions developed. It was therefore important to create a suitable taxonomy for the types of  
155 structures being studied. Conventionally, building damage has been assessed by separating the buildings into their various  
156 construction types (e.g. masonry, wood, steel, unreinforced and reinforced concrete). Charvet et al. (2014) noted differences  
157 in the performance of buildings with different construction types to tsunami impacts following the Tohoku event. However,  
158 port structures consist of both buildings and infrastructure, with the infrastructure of a highly specialised nature where the  
159 design and construction criteria are industry-specific. A more suitable approach then would be to classify port structures  
160 according to their industry.

161 Different types of port activities occupy the port area. Aside from the core business of terminal operations, the port is also host  
 162 to distribution centres and non-maritime activities. To the best of our knowledge, there is no standard industrial classification  
 163 for port activities. We therefore proposed a broad classification for the port activities found in Tohoku ports, according to the  
 164 general industry that they fall into (Table 2). Classification for non-maritime port industries was adapted from the terminologies  
 165 used by European Sea Ports Organisation (ESPO, 2016) for the various industrial sectors found in European ports. We used  
 166 Google Maps and Google Street View to identify the business nature of each company (industry type), commonly through the  
 167 name of the company at the time of the tsunami. We identified eight main port industries based on our proposed taxonomy.  
 168 Buildings in port industries commonly include administrative offices, control and maintenance buildings, warehouses and cold  
 169 storage. Industrial buildings are typically of steel or concrete construction. On the other hand, the types of port infrastructure  
 170 are diverse - ranging from small transformers to large loading cranes. Some common infrastructure found in each industry are  
 171 listed in Table 2, adapted from the descriptions provided by the AIR Construction and Occupancy Class Codes (AIR  
 172 Worldwide, 2019). Because of their diversity, port infrastructure vary widely in their construction and unlike buildings, it is  
 173 extremely challenging to classify them according to their construction nature. It is interesting to note, however, that several  
 174 industrial infrastructure are installed in support structures or housed in buildings. In the petrochemical industry, for example,  
 175 oil and gas are commonly stored in steel or concrete silos and tanks.

176  
177  
178 **Table 2.** Proposed classification for port activities found in the Tohoku region.

Industry type		Description of port activities
Maritime industries	Cargo handling industry	Cargo handling services such as loading and unloading of ships (stevedoring) as well as the handling of cargo on shore.  <u>Typical infrastructure: Loading and gantry cranes, storage yards, storage sheds, silos, chillers and warehouses (buildings).</u>
	Warehousing and distribution	Cold storage, warehousing and logistics support.  <u>Typical infrastructure: Storage sheds, tanks and silos.</u>
Non-maritime port-related industries	Chemical industry	Bulk chemical production e.g. alkane, propane and fertilisers.  <u>Typical infrastructure: Distillation towers, tanks, silos, conveyors, pipes, pumps, compressors, reactors, vessels,</u>



	<u>wastewater treatment systems, chemical separation columns, substations and open frame structures.</u>
Construction materials industry	Concrete and cement manufacturing. Asphalt and wood processing.  <b><u>Typical infrastructure:</u></b> <u>Rotary kiln/furnace, coal storage, grinders, mills, pre-heating towers, coolers, tanks, silos, conveyors, sorters and stackers.</u>
Energy-related industry	Coal power generation. Electric power generation and distribution.  <b><u>Typical infrastructure:</u></b> <u>Mills, power plants, substations, transformers, chimneys, boilers, generators, cooling towers, turbines, condensers, pumps and electricity transmission towers.</u>
Food industry	Seafood processing and food packaging. Feed manufacturing.  <b><u>Typical infrastructure:</u></b> <u>Ovens, cold storage (buildings), freeze dryers, tanks, mixers, conveyors, boilers and vessels.</u>
Manufacturing industry	Metal and alloy products. Plywood and paper products.  <b><u>Typical infrastructure:</u></b> <u>Grinders/refiners, chimneys, furnaces, silos, tanks, screens, conveyors, cranes, mills and rollers.</u>
Petrochemical industry	Oil depots, reserves and refineries.  <b><u>Typical infrastructure:</u></b> <u>Furnaces, distillation towers, crackers, compressors, condensers, vessels, tanks, silos and pipelines.</u>

### 180 **4.3 Maximum inundation depths**

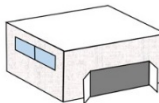
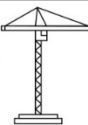
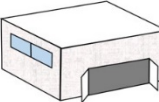
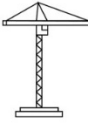
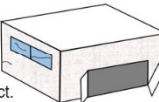

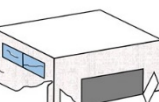


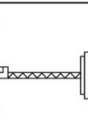
181 Various tsunami hazard intensity measures (e.g. inundation depth, flow velocity and force) have been used in literature to  
182 estimate structural fragility to tsunami impacts. Past studies ([Macabaug-Macabuag et al., 2016](#); Park et al., 2017; Attary et al.,  
183 2019) have shown that no single measure can fully characterise structural fragility to tsunami impacts as it is impossible to  
184 explain a complex phenomenon through a sole parameter. For the purpose of this study, observed maximum inundation depth  
185 was chosen as the representative intensity measure manifesting damage since depth is more easily estimated from field survey  
186 after tsunami events as compared to other flow values, which typically have to be simulated. Using observational data also  
187 minimises the uncertainty in intensity measure as compared to using simulated data (e.g. velocity and force).

188 Inundation characteristics were recorded and collected from a number of sources, namely tsunami trace heights by the Tohoku  
189 Tsunami Joint Survey Group (TTJS, 2011), MLIT survey, photographs, videos, eyewitness accounts and other reports  
190 (Leelawatt et al., 2014). The MLIT (2014) compiled all the maximum inundation depth values and building data into a single  
191 database. Inundation depth refers to the depth of floodwater above ground. Each building surveyed in the MLIT database is  
192 pegged with maximum inundation depth values, and where values were not available for some buildings (e.g. those that were  
193 washed away), they were interpolated from nearby buildings with inundation depth values (De Risi et al., 2017). Similarly, for  
194 buildings and infrastructure that were identified in this study, we interpolated inundation depth values from neighbouring  
195 surveyed buildings.

### 196 **4.4 Proposed damage classification scheme**

197 For the first time, a damage classification scheme for tsunami damage to port structures is being proposed (Fig. 3). The MLIT  
198 adopted a damage classification scheme for building damage assessment following the 2011 Tohoku tsunami (see Leelawatt  
199 et al., 2014). Naturally, subsequent studies that used the MLIT damage database to analyse damage and derive fragility  
200 functions followed the same classification scheme. The pitfalls of adopting the MLIT damage classification have been  
201 highlighted in several studies (Leelawat et al., 2014; Charvet et al., 2015; Charvet et al., 2017). Firstly, the MLIT classification  
202 consists of six damage states, which were found to have overlaps in their definitions (Leelawat et al., 2014; Charvet et al.,  
203 2015). The overlapping definitions might have resulted in buildings being wrongly classified when performing damage  
204 assessment. Ideally, damage states should be presented in a mutually exclusive and consecutive order (Charvet et al., 2015).  
205 Secondly, descriptions in the MLIT classification scheme do not distinguish between structural and non-structural damage.  
206 Therefore, the structural response of the buildings assessed is not being explicitly assessed. Additionally, by specifying the  
207 range of inundation depths associated with each damage state, such definitions allude to inundation depths being a condition  
208 of damage. This contradicts the objective of developing fragility functions as predictive models of damage. Over and above  
209 the limitations outlined, the MLIT damage classification solely describes damage to buildings, which is otherwise unsuitable  
210 for port structures.

211 To address the limitations of the existing damage classification of MLIT, we proposed a new damage classification for port  
 212 structures. This new classification scheme provides damage descriptions for both buildings and infrastructure. Degrees of  
 213 damage are classified into four levels (with damage state DS 0 being no damage), ensuring that the descriptions for each  
 214 damage state are mutually exclusive and in increasing order. Descriptions also include the expected serviceability of the  
 215 structure at each damage state. Pitalakis et al. (2014) argued that physical damages would reflect the expected serviceability  
 216 of the structure (condition for use) and its corresponding functionality (i.e. can its functions still be fulfilled?). The structural  
 217 integrity of port structures is also being considered. For instance, between DS 2 and DS 3, damage is distinguished by whether  
 218 it only affected non-structural components and/or roof (DS 2), or structural components such as columns and beams (DS 3).  
 219 We assumed that when the structural integrity of a structure is compromised, the structure would be removed.  
 220

Damage State	Damage Description	
	Buildings (B)	Infrastructure (I)
DS 0	<ul style="list-style-type: none"> <li>Little to no water penetration.</li> <li>Non-structural components (windows and door) and roof remain intact.</li> </ul> 	<ul style="list-style-type: none"> <li>No floodwater impacts on infrastructure.</li> </ul> 
	<i>Serviceability:</i> Ready for immediate use	
DS 1	<ul style="list-style-type: none"> <li>Water penetration.</li> <li>Non-structural components and roof remain intact.</li> </ul> 	<ul style="list-style-type: none"> <li>No visible damage from outside of infrastructure.</li> </ul> 
	<i>Serviceability:</i> Ready for immediate use but requires interior restoration, such as drying of floors and walls, repainting, repairs to plumbing and electric systems.	
DS 2	<ul style="list-style-type: none"> <li>Non-structural components and/or roof have sustained damage.</li> <li>Structural components are intact.</li> </ul> 	<ul style="list-style-type: none"> <li>Some damage to infrastructure, while foundation or base remains intact.</li> </ul> 
	<i>Serviceability:</i> Obvious repair works in the intermediate period after the tsunami. Operational only after repairs.	
DS 3	<ul style="list-style-type: none"> <li>Structural components (columns and beams) have sustained damage, or rackings have buckled and folded.</li> </ul> 	<ul style="list-style-type: none"> <li>Foundation or base of infrastructure has folded or buckled.</li> </ul> 
	<i>Serviceability:</i> Not repairable. Replacement or removal of building in the intermediate period after the tsunami.	
DS 4	<ul style="list-style-type: none"> <li>Total structural failure.</li> <li>Building has either overturned or slid from original position.</li> </ul> 	<ul style="list-style-type: none"> <li>Infrastructure has overturned or slid from original position.</li> </ul> 
	<i>Serviceability:</i> Not operational.	

221

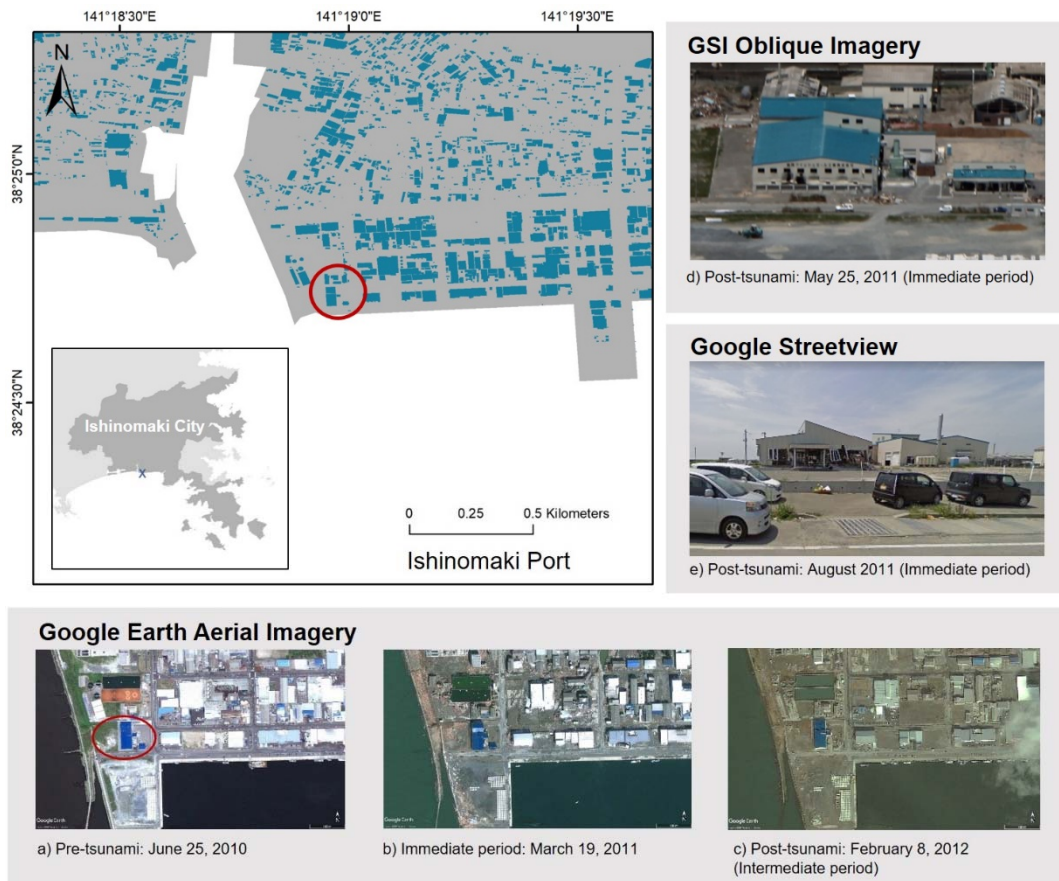
222 **Fig. 3.** Proposed new damage classification for port industries. Descriptions for damage to both buildings and non-building  
223 infrastructure are provided in the classification table. DS 1 and DS 2 are considered as non-structural damages, while DS 3  
224 and DS 4 are structural damages.

#### 225 **4.5 Damage assessment through spatio-temporal analysis**

226 A combination of free-to-use sources were used to inform our classification decisions when assigning damage states to  
227 individual port structures (Table 1). Port structures were assessed through the analysis of satellite imagery, using pre- and post-  
228 tsunami images from Google Earth engine and Geospatial Information Authority (2012a), as well as photographic  
229 interpretations of post-tsunami oblique images from Geospatial Information Authority (2012b). Pre- and post-tsunami images  
230 refer to observations made before 11 March 2011, and on and after 11 March 2011 respectively (Table 1). Apart from aerial  
231 and oblique images, we visually assessed the conditions of port structures through Google Street View images. Google Street  
232 View, a service available on Google Maps web, provides panoramic view of the landscape at a street level. An example of  
233 how a building or infrastructure was being assessed is illustrated in Fig. 4.

234 The three types of images (aerial, oblique and street view) provided different, yet complimentary, types of information. Aerial  
235 images were particularly useful in assessing washed away and collapsed structures (DS 4). Street View images were used to  
236 identify damage from façade level, which supplemented as “ground truth surveys”. The high-resolution imagery provided by  
237 Google Street View allowed us to pick up finer details such as structural and non-structural damage to port structures, which  
238 would otherwise be missing from aerial imagery. However, because Street View imagery was captured through vehicle-  
239 mounted cameras, the availability of these images are constrained by the accessibility of roads by the vehicle at the time of  
240 survey. Where imagery was not captured by Google Street View due to such constraints, we capitalised on the alternative  
241 views provided by GSI oblique images.

242 Advances in mapping technologies mean that temporal changes are also being captured and documented in these mapping  
243 applications. The time-slider functions on Google Earth engine and Google Street View web, as well as the date stamps on  
244 GSI images, allowed us to review temporal changes in the built environment. For images in Google Earth and Google Street  
245 View, different phases of the tsunami, i.e. pre-tsunami (before March 2011), immediately after the tsunami (up to 6 months  
246 after the tsunami) and the intermediate recovery phase (1 – 2 years), were all captured in the same point locations. With  
247 coordinates being embedded in the aforementioned data sources, we were also able to reference GSI aerial and oblique post-  
248 tsunami images to the same locations. The large amount of high-quality data provided by these image databases and mapping  
249 applications have been a large driver of our data collection in this study.



250

251 **Fig. 4.** A building (circled in red) in Ishinomaki Port has been selected to demonstrate how spatiotemporal damage assessment  
 252 had been conducted in this study. For every port structure, we reviewed four main sources of data (©Google Earth 2020,  
 253 ©Google Street View 2020, GSI Aerial and Oblique images) to estimate the level of damage sustained during the tsunami.

## 254 5. Model building

255 Fragility functions describe the probabilities of damage exceedance for a given intensity measure or flow characteristic. The  
 256 probability of damage exceedance can simply be expressed as:

257

$$PDS = P(ds \geq DS | IM)$$

258 , where  $ds$  is the observed damage state of a structure,  $DS$  the classification provided by the damage scale and  $IM$  the intensity  
 259 measure (Charvet et al., 2017). In the case of this study, tsunami inundation depth was used as an explanatory variable in the  
 260 prediction of structural damage probability. Typically, empirical tsunami fragility functions are constructed by fitting an  
 261 appropriate statistical model to post-tsunami damage data.

## 262 5.1 Evaluation of statistical models available

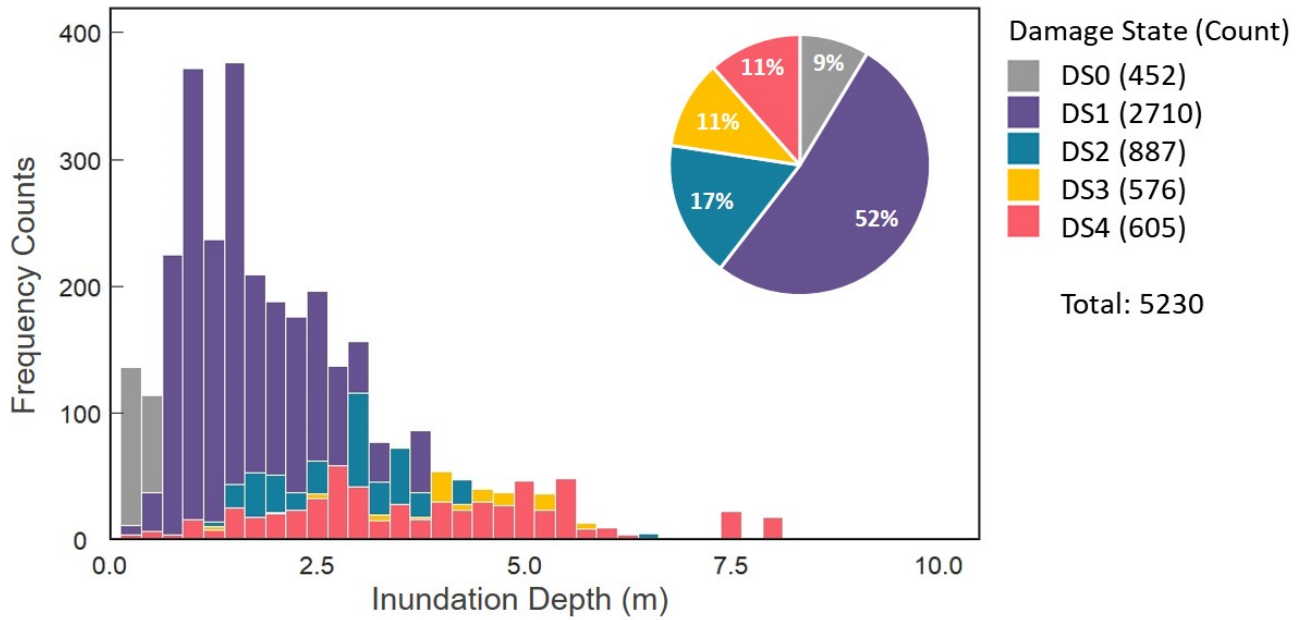
263 In recent years, a number of studies evaluated the suitability of various statistical models in representing tsunami damage to  
264 structures (Charvet et al., 2014; [Macabaug-Macabuag](#) et al., 2016; Charvet et al., 2017). Parametric (e.g. Ordinary Least Square  
265 regression, Generalised Linear Model or ordinal logistic regression models), semi-parametric (e.g. Generalised Additive  
266 Model) and non-parametric (e.g. Kernel Smoother) statistical model types are amongst the most commonly used. These  
267 statistical models are extensively reviewed in Rosetto et al. (2014), Lallemand et al. (2015), [Macabaug-Macabuag](#) et al. (2016)  
268 and Charvet et al. (2017), and readers are referred to these studies for a more comprehensive understanding of the advantages  
269 and disadvantages of using the various types of statistical models.

270 Generalised Linear Models (GLM), an extension of classical linear regression models, have been recommended as more  
271 reliable forms of fragility functions for the following reasons:

- 272 • Discrete probability distributions can be used to predict discrete responses (Charvet et al., 2017). This is especially  
273 important for categorical data (such as damage states), because it is statistically incorrect to assume that the difference  
274 between categories is linear/continuous, e.g. the difference between DS 1 and DS 2 holds the same meaning for the  
275 difference between DS 2 and DS 3 (Guisan and Harrell, 2000).
- 276 • Unlike classical linear regression models (e.g. ordinary least square regression) which assume either a normal or  
277 lognormal distribution, the response variable need not be normally distributed and can take on any of the exponential  
278 family distributions.
- 279 • It does not assume a linear relationship between the explanatory variable and response variable, but a linear  
280 relationship is assumed between the transformed response through a link function and the explanatory variables.
- 281 • Maximum likelihood estimation (MLE) is used rather than ordinary least squares to estimate the parameters. MLE  
282 has the advantage of explicitly reflecting the probability distribution of the random variable of interest.
- 283 • Overfitting of data can be avoided by using cross-validation analysis to determine optimal model parameter values.
- 284 • Model uncertainty can be quantified by supplementing the median of the response with confidence or prediction  
285 intervals.

## 286 5.2 Data exploratory analysis

287 The response variable is ordinal (in the sense that  $DS\ 0 < DS\ 1 < DS\ 2 < DS\ 3 < DS\ 4$ ). A visual inspection of the distribution  
288 of depth given damage data (Fig. 5) indicates non-normality, with the distribution skewed towards the right, indicating a  
289 lognormal transformation of inundation depth variable would be appropriate. Frequency counts of the damage data show that  
290 damage state (DS 1) makes up the majority of the dataset ( $n = 2710$ ), and DS 3 and 4 a much smaller proportion ( $n = 576$  and  
291  $n = 605$  respectively).



292

293 **Fig. 5.** Histograms of each damage state. Distribution of damage data indicates non-normality and DS 1 accounts for the  
 294 majority of the dataset. ~~Outliers exist in DS 3 and 4, with no damage states recorded for inundation values between 6 to 7.4~~  
 295 ~~metres. Outliers are not removed from the model, as they are legitimate observations and possible outcomes.~~

### 296 5.3 Selection of a suitable statistical model

297 An ordinal logistic regression model, an ordinal and logistic recourse of GLMs, is adopted. It has the additional advantage of  
 298 accounting for and maintaining the ordered nature of damage-state data. As this model recognises the ordered nature of the  
 299 damage states, overlapping pathways of the fragility functions can be avoided (Charvet et al., 2017). Overlapping fragility  
 300 functions, as is common when fitting separate GLMs, may unwittingly imply that the probability of a higher damage state (e.g.  
 301 DS 4) being exceeded is higher than that of a lower damage state (e.g. DS 3) as inundation depth increases. Ordinal models  
 302 also make full use of the ranked data rather than simplifying it into binary exceedance and non-exceedance, and therefore  
 303 preventing the loss of information (Ananth and Kleinbaum, 1997).

304 The dependence of the response variable DS on predictor variable X can then be represented as follows

$$305 P_{DS} = P(ds \geq DS_i | X_j)$$

306 , where  $DS_i$  refers to the  $i_{th}$  damage state,  $j$  the specified predictor (IM) or combination of predictors. The model relates the  
 307 probability of the outcome,  $P_{DS}$ , to all explanatory variables  $(X_1, X_2, \dots, X_j)$  through a linear predictor. There are three basic  
 308 components to any GLM, and Table 3 describes the components in the context of the ordinal logistic model used in this study.  
 309

Random Component	<i>The probability distribution of the response variable.</i>
	A multinomial distribution is assumed for the cumulative probabilities in an ordinal logistic regression model.
Systematic Component	<i>The explanatory variable (<math>X_j</math>) or the linear combination of the explanatory variables (<math>X_1, X_2, \dots, X_j</math>) in creating the linear predictor e.g. <math>\beta_0 + \beta_1 X_1, \beta_2 X_2 + \dots + \beta_j X_j</math>, where <math>\beta_0</math> and <math>\beta_{1,j}</math> are transformed constant and regression coefficients through maximum likelihood estimation.</i>
Link function	<i>The link between random and systematic components.</i>
	Describes how the cumulative probability $P_{DS_i}$ of the expected outcome for any damage state $DS_i$ relates to the linear predictor of explanatory variables $X_j$ . In this instance, the link function chosen takes on a logit form $g$ where
	$g(P_{DS_i}) = \log\left(\frac{P_{DS_i}}{1 - P_{DS_i}}\right)$
	, with
	$P_{DS_i} = P(ds \geq DS_i   X_j) \quad \forall i \in (1, \dots, I)$
	Therefore, the dependence of the response variable DS on the linear predictor can be re-expressed as
	$\log\left(\frac{P_{DS_i}}{1 - P_{DS_i}}\right) = \beta_{0,i} + \beta_1 X_1 + \beta_2 X_2 + \dots + \beta_j X_j$
	$\log\left(\frac{P_{DS_i}}{1 - P_{DS_i}}\right) = \beta_{0,i} + \sum_{j=1}^J \beta_j X_j$
	The corresponding regression coefficients $\beta_{1,j}$ in the link function are fixed across every damage state except for the intercept, so as to maintain the order of the response categories.



312 The conditional probability  $P(ds \geq DS_i | X_j)$  is a common vector of regression coefficients  $\beta$ , which connects probabilities for  
 313 varying levels of damage. When expressing the cumulative probabilities of each damage state as separate curves, the  
 314 relationships between damage states in increasing order of severity are defined as follows:

$$315 \quad P_{DS} = P(ds = DS_i | IM = X_j) = \begin{cases} 1 - P(ds \geq DS_i | X_j) & i = 0 \\ P(ds \geq DS_i | X_j) - P(ds \geq DS_{i+1} | X_j) & 0 \leq i \leq N_{DS} \\ P(ds \geq DS_i | X_j) & i = N_{DS} \end{cases}$$

316

317 , where  $N_{DS}$  refers to the number of damage states, including DS 0 (Macabaug-Macabuag et al., 2016).

## 318 6. Model evaluation

### 319 6.1. 10-fold cross-validation

320 Model accuracy was used as a quantitative indicator of the performance of our models. We wanted to assess the goodness-of-  
 321 fit of the models and determine its predictive ability. It was difficult to test the predictive ability of our models where there  
 322 were no further samples to test with. In order to optimise model design while preventing overfitting, the cross-validation  
 323 method was applied to evaluate the prediction accuracy of our models. Cross-validation techniques make use of the available  
 324 dataset by dividing them into two subsamples – one to train the model and the other to predict the model on.

325 One cross-validation technique is K-fold, where the dataset is divided into K number of approximately equal-sized subsets as  
 326 illustrated in Fig. 6a. One subset is taken out as a test set for validation, and the remaining  $K - 1$  subsets are then used to train  
 327 a model. This hold-out method is then repeated for K number of times, with a new subset being used as a test set in each  
 328 iteration. Only after all K models are fitted, statistics of the model performance are tabulated. For the purpose of this study, a  
 329 10-fold cross-validation approach was taken.

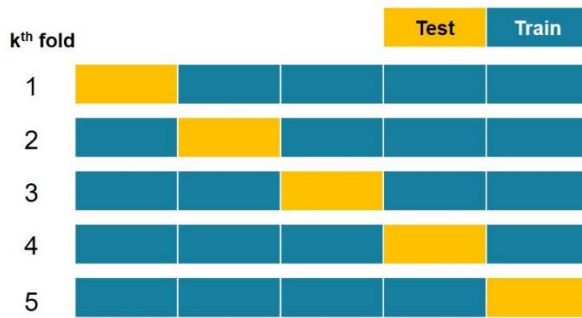
330 The accuracy of a model is determined by the proportion of correctly classified responses. When applied to the k-fold  
 331 technique, the fitted model is used to predict response on the held-out  $k^{\text{th}}$  subset in each iteration. The recorded response is  
 332 tabulated against actual observations in the  $k^{\text{th}}$  subset and a confusion matrix is constructed as demonstrated in Fig. 6b. The  
 333 diagonal of the confusion matrix represents the sum of correctly predicted response, the proportion of correctly classified  
 334 response is then calculated by

$$335 \quad Accuracy = \frac{\text{Sum of correctly predicted response}}{\text{Sum of total observations}}$$

336

337 Accuracies are recorded in each iteration of the K-fold, and the mean and standard-deviation of the tabulated accuracies are  
 338 taken to assess the predictive ability of the model. All statistical analyses and modelling in this study were carried out using  
 339 the statistical software R (R Core Team, 2020).

### a) K-fold cross-validation



### b) Confusion matrix for accuracy

		Predicted			
		DS 1	DS 2	DS 3	DS 4
Actual	DS 1	30			
	DS 2		20		
	DS 3			8	
	DS 4				9

Example of  $k^{\text{th}}$  in K number of folds

340

341 **Fig. 6.** (a) An example of a 5-fold cross-validation technique for the purpose of illustration. The same dataset can be folded  
 342 into 5 equal sizes, and one fold is held-out for testing and the remaining 4 folds are used to develop a training model to predict  
 343 the accuracy of the training model. This is repeated 5 times, with accuracies being tabulated in each iteration. (b) Accuracy  
 344 table (confusion matrix) is produced in each iteration of the k-folds. The sum of the diagonal in the table is divided by the sum  
 345 of observations to get the percentage of accuracy in the  $k^{\text{th}}$  fold.

## 346 6.2 Quantification of uncertainty

347 The fragility functions, when presented as curves or plots, represent the expected value of the response variable. Therefore,  
 348 they represent only a sample estimate of the population values. Statistical variations of the fragility functions can be accounted  
 349 for by estimating the confidence intervals. In this study, we adopted bootstrap-based confidence intervals to estimate the  
 350 uncertainty in estimation or prediction. The bootstrap method treats the original dataset of values as a realised sample from the  
 351 true population and does not make any assumptions about the underlying distribution of the population parameters (Yung and  
 352 Bentler, 1996). Values from the original dataset are resampled repeatedly, with replacement. This was done for 1000 iterations,  
 353 with the predicted logit computed in each iteration. To derive a 95% confidence band, the 2.5<sup>th</sup> and 97.5<sup>th</sup> quantiles of the 1000  
 354 estimates were drawn at each inundation depth interval (0.01m).

## 355 7. Results

### 356 7.1. Damage database for port structures

357 To characterise the vulnerability of assets in various port industries, damage assessment was performed for buildings and  
 358 infrastructure in the Tohoku region. We compiled damage information on port structures into a database, which is available  
 359 online through an unrestricted data repository (DR-NTU) hosted by Nanyang Technological University  
 360 (<https://doi.org/10.21979/N9/OTZMT1>) (Chua et al., 2020).

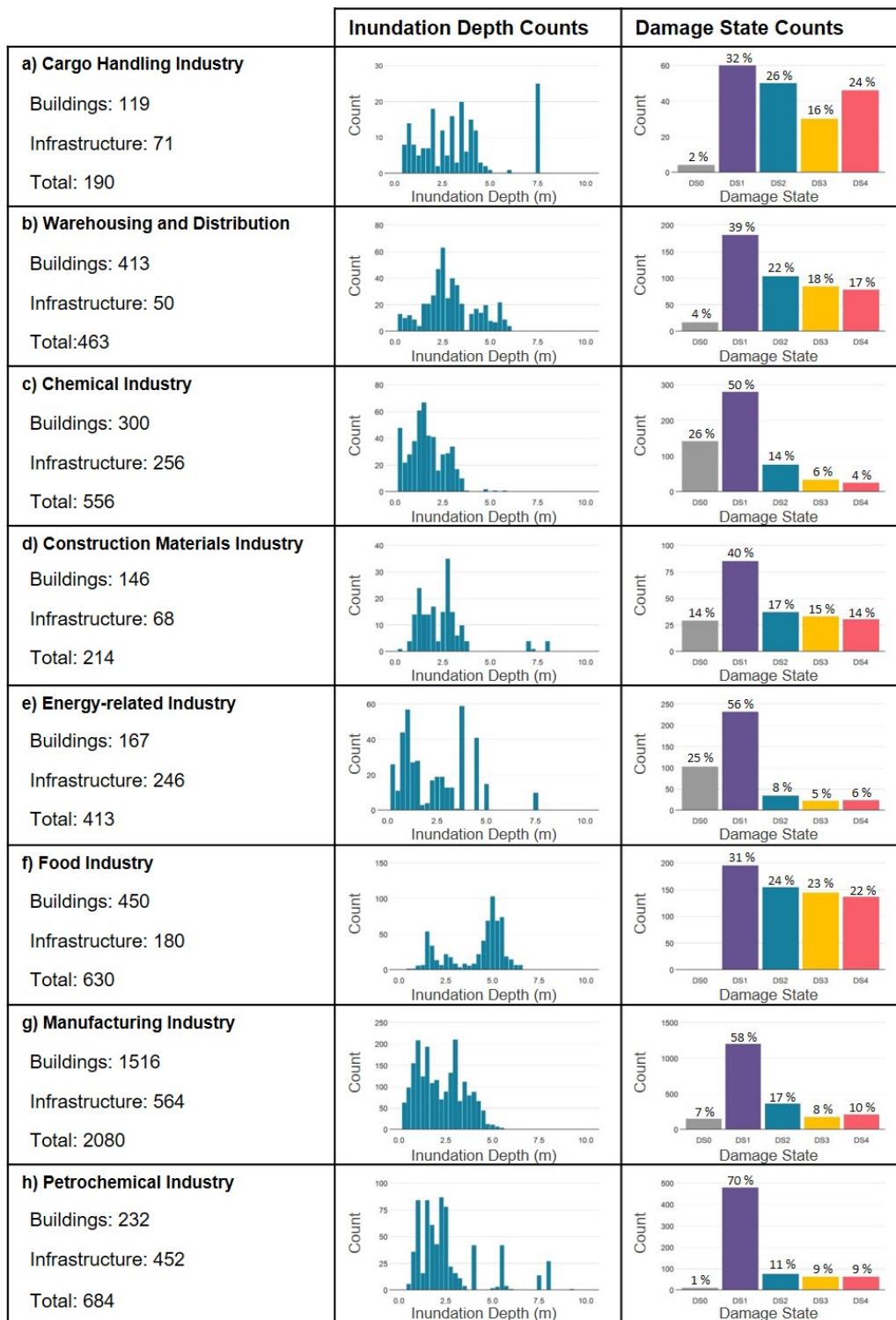
361 The port damage database consists of 5,230 port structures, of which 3,343 are buildings and 1887 are infrastructure. The port  
 362 structures were identified in six case study ports, across eight port industries. The damage dataset show that most port structures

363 sustained minimal structural damage classified as damage state DS 1 (Table 4). Consistently for all port industries, the majority  
 364 of the observed damage corresponds to DS 1 (Fig. 7.) Notably, many industries such as chemical, petrochemical and energy-  
 365 related industries sustained minimal structural damage mainly due to flooding at DS 1, which only required some clean up and  
 366 interior restoration and remained mostly operational after restoration. On the other hand, cargo handling and food industries  
 367 sustained a wide range of damage from minimal damage (DS 1) to total damage (DS 4), corresponding to nearly all damage  
 368 states. Tsunami floodwaters at depths of less than 5 metres inundated most port structures. In extreme cases, inundation depths  
 369 affecting port structures reached as high as 7.5 metres. The minimum recorded inundation depth was 0.1 m.

370

371 **Table 4.** Summary of port structures identified in the various ports, sorted according to their industries.

	North Tohoku		South Tohoku				Total
	Hachinohe	Kuji	Ishinomaki	Sendai	Soma	Onahama	
Cargo Handling Industry	31	9	31	32	25	62	190
Warehousing and Distribution	111	16	175	105	39	17	463
Chemical Industry	236	-	208	27	85	-	556
Construction Materials Industry	29	20	20	99	9	37	214
Energy-related Industry	125	-	-	104	134	50	413
Food Industry	12	37	430	151	-	-	630
Manufacturing Industry	1010	60	587	279	144	-	2080
Petrochemical Industry	202	41	38	324	-	79	684
<b>Total</b>							5230



372

373 Fig. 7. Data attributes of the port industries affected by the 2011 Great East Japan tsunami.

## 374 7.2 Damage fragility functions for port industries

375 Damage fragility functions were produced for eight major port industries as depicted in Fig. 8. Individual fragility curves were  
376 plotted for each damage state and the solid lines represent the probabilities of a structure exceeding each damage state given a  
377 range of inundation depths and the shaded regions their corresponding 95% confidence intervals.

378 The fragility functions (Fig. 8) suggest that chemical, cargo handling, and construction materials industries are more  
379 vulnerable. Higher probabilities of damage exceedance are reached at a more rapid rate as compared to other industries. In  
380 contrast, energy-related industry and warehousing and distribution are showing a gentler incline in damage probability for  
381 higher levels of damage (DS 3 and DS 4), indicating a greater resistance to tsunami impacts. A key assumption of fragility  
382 studies and of this study is that damage is directly related to the properties of the elements at risk. Thus, aside from tsunami  
383 intensity measures, the composition and structural design of each industry could determine the differences in vulnerabilities.  
384 For example, power plants (energy-related industries) and warehouses are structurally robust by design. Most heavy equipment  
385 found in power plants is normally supported in large reinforced concrete foundations or housed in large steel structure buildings  
386 (Cruz and Valdivia, 2011) and is therefore more resistant to tsunami loads. Likewise, many warehouses in the studied ports  
387 were reinforced concrete buildings with their warehouse floor raised above road levels, which increased the height of non-  
388 structural elements (e.g. docks and doors) relative to tsunami inundation. Comparatively, chemical facilities typically consist  
389 of more fragile components which are not part of the primary load resisting systems such as pipelines, pumps, compressors  
390 and tanks, and they are extremely vulnerable to damage from tsunami inundation and forces. As observed in the 2011 event,  
391 hydrodynamic and hydrostatic forces from the tsunami resulted in the breaking of pipe connections, floating tanks and  
392 overturning of unanchored infrastructure (Krausmann and Cruz, 2013). Meanwhile in cargo handling facilities, loading and  
393 unloading infrastructure were ~~creas~~ mostly anchored, but instances of cracked pavements and damaged crane rail foundations by  
394 the earthquake and tsunami were reported to result in the derailment and collapse of cranes (Technical Council on Lifeline  
395 Earthquake Engineering, 2017). ~~Nonetheless, other factors such as debris impact and proximity to shoreline should not be  
396 discounted when considering the differences in the response of each industry to tsunami impacts.~~

397 Other factors such as debris impact and proximity of the structure to the shoreline should not be discounted when considering  
398 differences in the response of each industry to tsunami impacts. Tsunami-borne debris can contribute significantly to structural  
399 damage. This issue is particularly present in port facilities, where ships, containers, mobile equipment, construction materials  
400 such as wood logs and concrete objects can impact on structures. Port structures are typically of more robust construction and  
401 therefore, they act as barriers in the path of debris motion for as long as inundation depth is lower than the structure height  
402 (Reese et al., 2007; Naito et al., 2014). As a result, they are more likely to be subjected to damage from debris impact (Charvet  
403 et. al., 2015). While debris impact is location-specific and does not affect all areas in the same ways, some industries may be  
404 more susceptible to debris impact than others. For example, in cargo handling and construction materials industries, where  
405 mobile large objects such as containers and wood logs are stored in open yards, there is a higher concentration of potential  
406 debris and therefore, a higher debris delivery potential (Naito et al., 2014). Kumagai (2013) surveyed the post-mortem dispersal

407 of containers after the 2011 Tohoku event and found that containers, which were not washed out to sea, were mostly dispersed  
408 within the terminals where they were located in. Many of these containers were also found to be concentrated around buildings  
409 surrounding the container yards without travelling further inland (Kumagai, 2013; Naito et al., 2014), which suggests that  
410 damage sustained to structures within these facilities are more likely a consequence of the combined effect of debris impact  
411 and tsunami flow than hydrodynamic force alone.

412

413 For each damage state, we considered the minimum depths where damage exceedance probability reaches near 1 or becomes  
414 nearly certain. Minimum damage (DS 1) is almost certain at 2.5 m consistently for all industries except energy-related industry.  
415 DS 1 occurs when there is water penetration into the building and interior restoration is required (Fig. 3). Logically, water  
416 penetration into buildings would be expected from 0.45 m since buildings are required to be constructed 0.45 m above road  
417 level as specified by the Building Standard Law of Japan (Building Centre of Japan, 2013). Threshold depths for DS 1 might  
418 have occurred at 2.5 m because of the aggregation of data for both infrastructure and buildings. We observed that there were  
419 many buildings (especially warehouse) and infrastructure such as storage tanks and silos that were elevated above ground and  
420 therefore, the number of exposed assets at lower inundation depths were reduced. The trend for other damage states is however  
421 not obvious and it is difficult to pinpoint minimum depth values where damage becomes certain.

422 A threshold value is said to be reached when damage curves from all states of damage converge at the probability of near  
423 100%. Key threshold value can be defined as the parameter (in this case, inundation depth) criteria at which DS 4 (collapse)  
424 becomes certain. Earlier studies of the 2011 Great East Japan tsunami (Suppasri et al., 2013; Charvet et al., 2014) examined  
425 the key threshold values for buildings, using damage data provided by MLIT. Suppasri et al. (2013) identified 2 m to be the  
426 key threshold value for all building types. More recent analysis found inundation depth thresholds to differ between  
427 construction types: from 2 m for wooden buildings (Charvet et al., 2014) to more than 10 m (Charvet et al., 2015) for steel and  
428 reinforced concrete construction types. Similar patterns have emerged in the present analysis. The near 100% probability of  
429 collapse occur at inundation depth exceeding 10 m for all industries. As such we were unable to quantify the key threshold  
430 values for collapse for port industries. There are several possible reasons for this observation. Two likely explanations stand  
431 out. The first being port structures are structurally much more resistant to tsunami loads than regular low-rise buildings because  
432 industrial buildings and structures are designed to withstand greater loads, including but not limited to dead loads, live loads,  
433 wind and earthquake loads. Therefore, greater tsunami inundation depths are required to overcome the resistance of port  
434 structures. A second possible explanation is that inundation depth alone is insufficient to explain damage, although it provides  
435 a first indication.

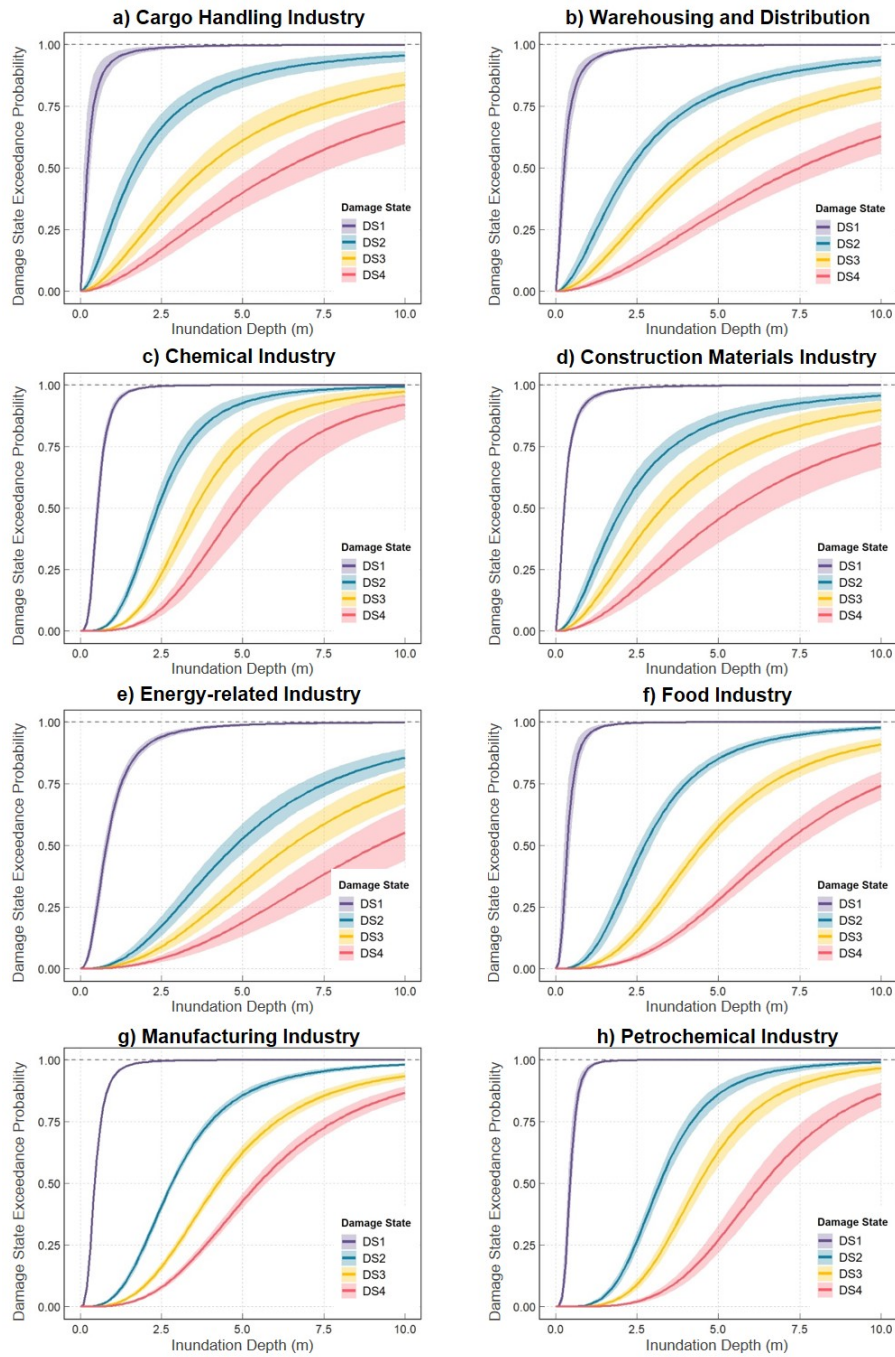
436 The effects of uncertainty were quantified through the construction of confidence intervals around the mean-median of the  
437 resulting probabilities. Confidence intervals around DS 1 are consistently narrow in width for all industries (Fig. 8), which  
438 could be associated with its large sample size. Contrastingly, for higher levels of damage (DS 3 and DS 4), confidence intervals  
439 tend to widen towards higher inundation depths. An observation made in the process of damage data collection through  
440 photographic interpretations was that many structures sustained very little damage despite high inundation depth values, which

441 explains the smaller sample sizes and therefore wider confidence intervals for DS 3 and DS 4 at higher depth values. In the  
442 same way, industries with the widest confidence intervals such as cargo handling industry and construction materials industry  
443 tend to have smaller sample sizes. By contrast, variabilities around the median curves tend to be smaller for the manufacturing  
444 industry, food industry, warehousing and distribution and petrochemical industry due to their larger sample sizes.

445 These findings can alternatively be justified by the effects of debris impact. A couple of studies (e.g. Charvet et al., 2015;  
446 Macabuag et al., 2015) have found the inclusion/omission of debris impact to have an effect on fragility models. Macabuag et  
447 al. (2015) demonstrated that models that include regression parameters considering debris impact have a better fit (statistically  
448 more significant) than models that do not. The authors also argued that the omission of debris information will likely introduce  
449 systematic bias to the fragility models. In this study, debris impact has not been explicitly considered in the development of  
450 fragility models, though it could be a source of uncertainty in our fragility models. Intuitively, structures that were damaged  
451 by debris would fall into higher damage states and likely experienced higher tsunami intensity values (i.e. depth and velocity).  
452 By neglecting debris impact, it is unsurprising that confidence intervals tend to widen towards higher depth values for DS 3  
453 and DS 4 (Fig. 8). Similarly, by neglecting debris information, fragility functions derived for industries, such as cargo handling  
454 and construction materials industries, that are more heavily impacted by the debris-related damage are expected to have greater  
455 uncertainties.

456

457



458

459 **Fig. 8.** Fragility curves with 95% confidence bands for port industries identified in this study. Chemical, cargo handling and  
 460 construction materials industries appear to be more vulnerable to tsunami inundation depths, while petrochemical and  
 461 warehousing and distribution industries have lower damage probabilities for the same inundation depths. Wider confidence  
 462 bands imply greater variability in uncertainty and could be results of smaller sample sizes.



## 463 8. Discussion

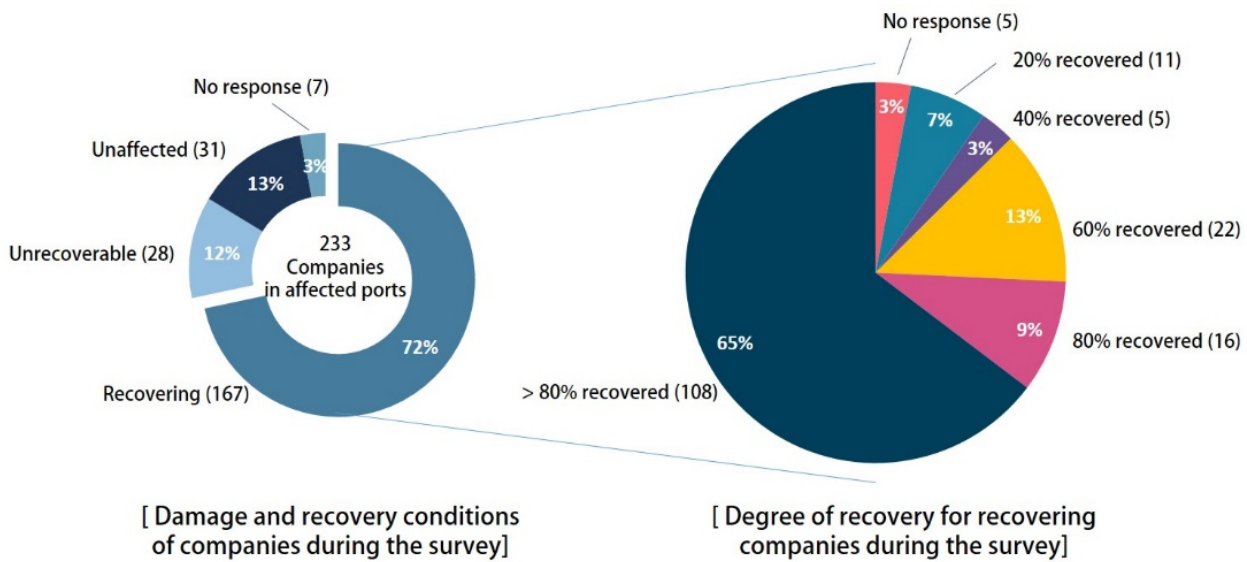
### 464 8.1 Comparison of damage dataset with functionality of port industries post-tsunami

465 We compared the damage database with existing literature to validate our observations. Most of the existing literature are  
466 either limited to descriptive analysis of damage to port facilities or are not available in English. We found only one study to  
467 be comparable with this study, in terms of the quantification of damage to port industries. A post-2011 tsunami survey was  
468 carried out by the Tohoku Regional Development Bureau (MLIT, 2011) between October and November, 2011. We considered  
469 the survey period as the intermediate period for reconstruction after the tsunami. The survey is a questionnaire survey on the  
470 recovery status of companies in tsunami-affected ports, including ports outside of our study sites. 226 of the 233 companies  
471 found in the affected ports responded to the survey. Findings from the survey were adapted from MLIT (2011) and we have  
472 translated them into English (Fig. 9).

473 We drew comparisons between the recovery status of the companies affected (MLIT survey) and the serviceability of port  
474 structures at each damage state (this study). It is difficult to make a direct comparison between the two. While port structures  
475 are the physical components of these companies, port structures and companies are inherently different entities. Therefore, an  
476 assumption made here is that the serviceability of port industries is indicative of the recovery status of the companies surveyed  
477 in the MLIT survey.

478 13% of the companies were found to be unaffected by the tsunami (Fig. 9), which marks a good agreement with our study  
479 where port structures sustaining no damage (DS 0) makes up 9% of the dataset (Fig. 4). In addition, approximately 12% of the  
480 companies found to be unrecoverable, which we assume to correspond to damage state DS 4 (11%) in our study. The MLIT  
481 survey found 72% of the companies to be in various stages of recovery during the survey and a majority (46.8%) of the  
482 companies were almost fully recovered (> 80% recovery) in the intermediate phase. Similarly, a large proportion (52%) of our  
483 damage data falls into DS 1 where port structures can be operational almost immediately after tsunami (Fig. 3). It is  
484 challenging, however, to draw parallel between the degrees of recovery with the damage states presented in this study. We  
485 stress that this approach is a relative measure of the validity of our dataset and damage assessment. Nonetheless, we can infer  
486 that damage observations made from photographic interpretations in this study are rather similar to actual observations.

487



488

489 **Fig. 9.** Damage conditions and degrees of recovery of companies in the tsunami-affected ports of Hachinohe, Kuji, Miyako,  
 490 Kaimaishi, Ofunato, Ishinomaki, Sendai-Shiogama, Soma and Onahama. 65% of the recovering companies were almost close  
 491 to full recovery (>80%) at the time of the survey. Adapted and translated from MLIT (2011).

492 **8.2 Fragility models and their classification accuracies**

493 Using the 10-fold cross validation technique, we evaluated the prediction accuracies of our models. Mean accuracies and their  
 494 standard deviations for each industry are illustrated in Table 5. Port structures have an overall accuracy of 59%. The  
 495 petrochemical industry, energy-related industry, chemical industry and manufacturing industry display higher accuracies –  
 496 75%, 70%, 69% and 64% respectively. In contrast, warehousing and distribution industry, cargo handling industry and food  
 497 industry display lower prediction accuracies – 40%, 38% and 28% respectively.

498 We looked at the underlying nature of our datasets to better understand the differences in accuracies. The petrochemical  
 499 industry, energy-related industry, chemical industry and manufacturing industry display higher accuracies and are represented  
 500 by large sample sizes (Fig. 7). On the contrary, the cargo handling industry is represented by only 190 data points. However,  
 501 because the food industry is represented by a large sample size but seemingly displays very low accuracy, we were unable to  
 502 conclude that sample size has an influence on the accuracies of the fragility models. In addition, the three industries  
 503 (warehousing and distribution, cargo handling and food industries) which display low accuracies are well represented across  
 504 all damage states.

505 The intrinsic differences between industries could have an effect on reducing accuracies. The composition of buildings and  
 506 infrastructure differ from industries to industries. For instance, cargo handling industry, which displays lower accuracy,  
 507 typically consists of mobile equipment such as cranes and conveyors as well as temporary transitional storage and components  
 508 such as chillers and tanks. Damage to transient port structures as such may be reflected in the damage data as part of the overall

509 assessment and introduce noise to the damage data, thus reducing model accuracy. In addition, the structural design of port  
 510 structures may vary between facilities of the same industry. For example, warehouses in the studied ports were mostly  
 511 reinforced concrete buildings, but some were made of mixed materials such as reinforced concrete foundations with light metal  
 512 or masonry walls. Whereas power plants (energy-related industry) and petrochemical industry are consistent in construction  
 513 material and more robust by design, which perhaps explain their higher accuracies. Thus, variability between port structures  
 514 of the same industries can also impact accuracy if those variables are not accounted for in the models. Second-order factors  
 515 beyond flow regime such as debris impact and proximity to the shoreline could also have an effect on model accuracies.  
 516

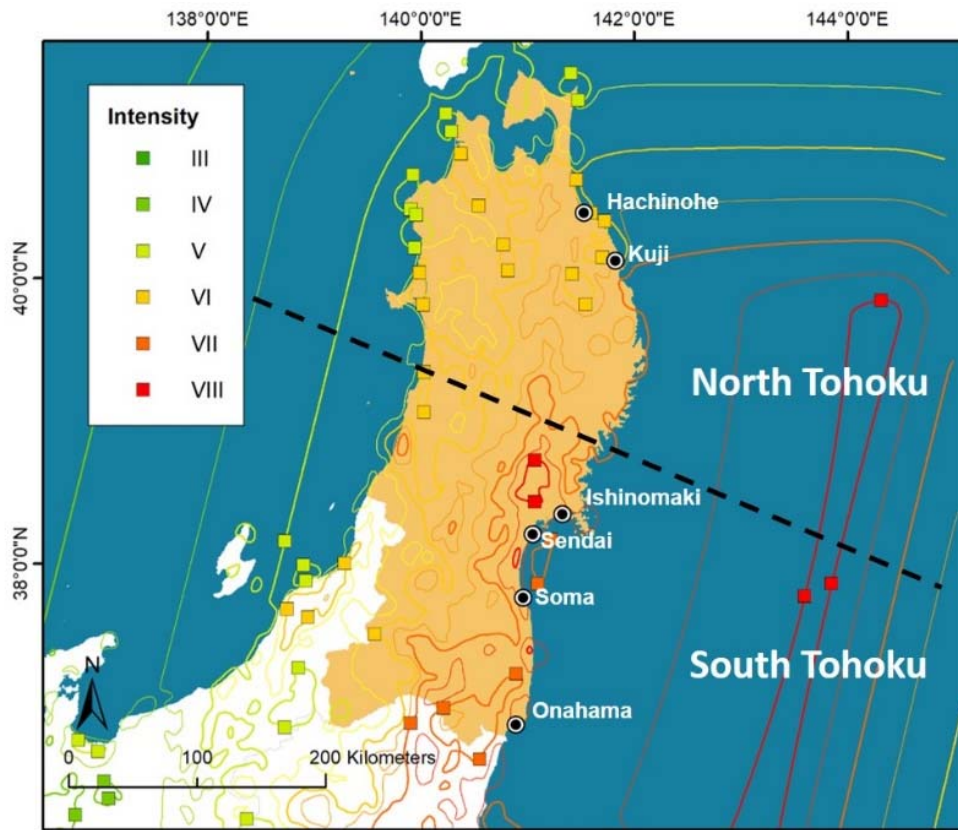
517 Another possible explanation is that many assets might have sustained extensive damage from earthquake activities such as  
 518 ground motion and liquefaction prior to the tsunami, as was observed by Kazama and Noda (2012). A preliminary inspection  
 519 of the damage dataset indicated a greater representation of data from ports that have experienced stronger ground motion for  
 520 the following industries – food, cargo handling and warehousing and distribution (Table 4). On the other hand, industries that  
 521 display higher accuracies have a greater data representation from ports that were not as severely affected by ground motion.  
 522 The significance of this relationship between the effects of the preceding earthquake and the damage observed is further  
 523 investigated in the proceeding section.

524 For most industries, our models performed better in terms of their classification accuracies as compared to fragility models  
 525 developed for buildings using the MLIT damage classification, which were found to have an accuracy of 52% (Leelawat et  
 526 al., 2014). As this is the first time tsunami damage is being quantified as a response of inundation depth for port industries, we  
 527 have no other models that we could use for comparison.  
 528

529 **Table 5.** Mean accuracies and standard deviations of accuracies of the various port industries.

Industry Type	Mean Accuracy	SD Accuracy
Cargo Handling Industry	0.374	0.221
Warehousing and Distribution	0.397	0.198
Chemical Industry	0.687	0.300
Construction Materials Industry	0.502	0.285
Energy-related Industry	0.707	0.245
Food Industry	0.283	0.204
Manufacturing Industry	0.638	0.249
Petrochemical Industry	0.746	0.218
All Industries (Whole Tohoku)	0.587	0.203

530



532

533 **Fig. 10.** Mercalli intensities (MI) recorded by United States Geological Survey (USGS, 2020) for the Great East Japan  
 534 earthquake and tsunami. Earthquake intensities differ between the northern (MI VI) and southern (MI VII - VIII) regions of  
 535 Tohoku. North Tohoku experience less effects from ground shaking than in the South.

536

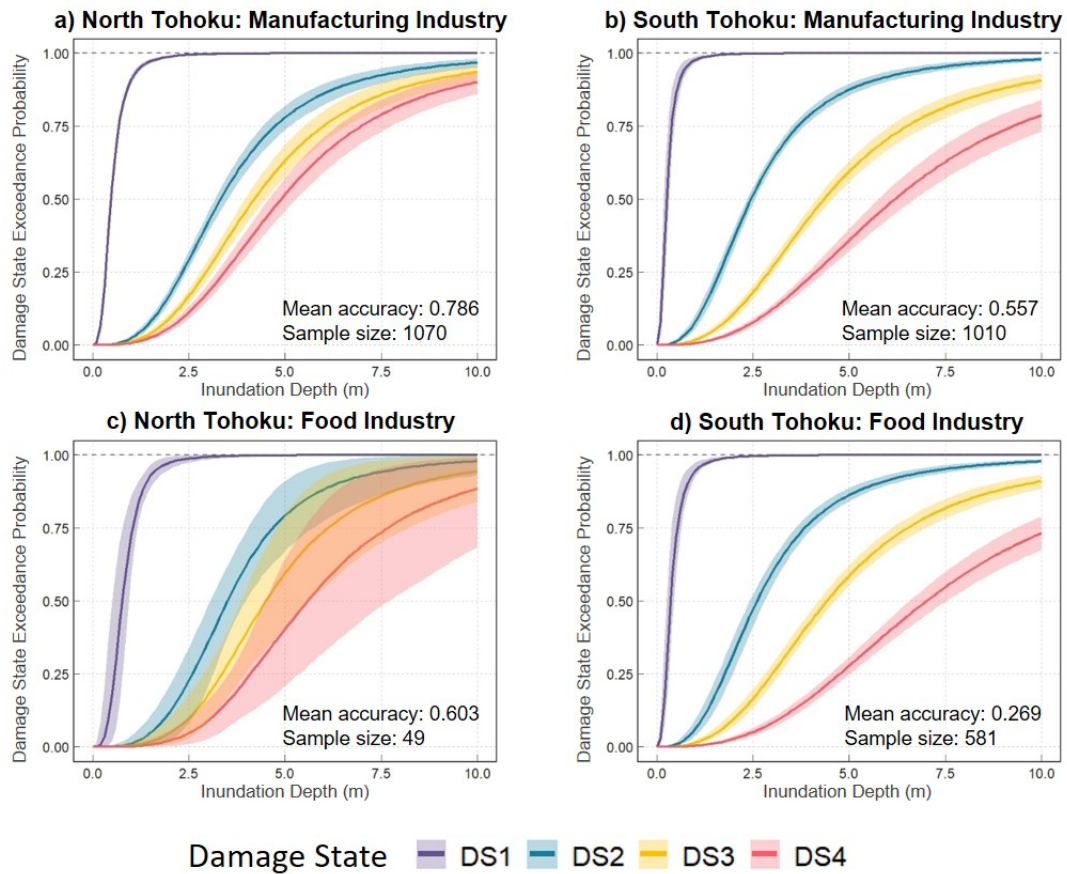
537 One of the concerns raised in the process of this research was the effect of ground motion, which preceded the arrival of the  
 538 tsunami, on asset damage. The effect of ground motion on damage to coastal structures was studied by Sugano et al. (2014).  
 539 The authors noted that in the northern Tohoku region, only little damage was sustained due to ground motion and the damage  
 540 observed was to a greater effect due to tsunami inundation. On the other hand, damage due to ground motion was substantially  
 541 greater in southern Tohoku region, more specifically coastal areas south of Miyagi Prefecture. Similar observations were made  
 542 by Okazaki et al. (2013), whom conducted surveys in Ishinomaki and Sendai ports and found that the two sites were exposed  
 543 to both severe ground motions and great tsunami wave heights. Kazama and Noda (2012) have also highlighted the possibilities  
 544 of liquefaction prior to the arrival of the tsunami but noted the impossibility of identifying locations of which liquefaction had  
 545 occurred after the tsunami.

546 To assess if ground motion-induced damage affects the accuracies of our models, we separated the damage data according to  
547 the locations of ports (between northern Tohoku and southern Tohoku regions). The ports of Hachinohe and Kuji fall within  
548 the northern region, and the ports of Ishinomaki, Sendai, Soma and Onahama are located within the southern region (Fig. 10).  
549 We selected two industries to capture the effect of ground motion, instead of using the entire dataset since it has the effect of  
550 aggregating data from different industries and hence neglect differences in their physical characteristics. The manufacturing  
551 industry was considered because of its high prediction accuracy and its large sample size. The food industry was also  
552 considered due to its poor prediction accuracy – we wanted to examine if pre-earthquake activities might explain the poor  
553 prediction ability of the fitted model.

554 Damage data for both industries was split into two sites (North and South Tohoku). For each dataset, an ordinal regression  
555 model was fitted and its response was captured in a 10-fold cross-validation. The resulting fragility models and their mean  
556 accuracies are shown in Fig. 11. We observe that port structures in South Tohoku tend to reach high probabilities of non-  
557 structural (DS 1 and DS 2) damage at lower inundation depths than structures in North Tohoku. This suggests that earthquake  
558 damage might have weakened structures prior to the tsunami, leading to a steeper incline in damage probabilities as compared  
559 to structures in North Tohoku. However, at higher levels of damage (DS 3 and DS 4), ground shaking appears to have had less  
560 influence on damage. For both industries in the northern region, models depict a smaller initial increase in damage for higher  
561 levels of damage DS 3 and DS 4 but probabilities incline more rapidly at higher inundation depths. The opposite holds true for  
562 both industries in the southern region, i.e. damage probability for DS 3 and DS 4 incline at a slower rate at higher inundation  
563 depths implying that a larger depth is required to induce structural damage (DS 3) and collapse (DS 4). Ground shaking  
564 therefore only influenced lower levels of damage, tsunami inundation and flow characteristics still had a greater influence on  
565 higher levels of damage.

566 The mean accuracies of using only datasets from North Tohoku are significantly higher than those of South Tohoku datasets.  
567 It appears that the aggregation of datasets from the two environments has the effect of averaging the mean accuracies for the  
568 whole region (Table 5, Fig. 11). It suggests that damage sustained by port structures in the Southern Tohoku region was  
569 influenced by the compound effects of earthquake and tsunami loads. Inundation depth alone is not sufficient to explain the  
570 damage observed. However, as Charvet et al. (2014) pointed out, it is difficult to distinguish the extent to which buildings had  
571 already been affected by earthquake damage prior to the arrival of the tsunami. Therefore, it was difficult to separate the effects  
572 of ground motion and liquefaction when we developed our fragility models.

573 There are other factors such as debris impact, the effect of shielding and local characteristics of the built environment that may  
574 have influenced the results observed (Tarbotton et al., 2015). Regardless, we note that while the fragility model developed for  
575 food industry using only data from the North has an improved mean accuracy, there is a substantial increase in the uncertainty  
576 of the model (Fig. 11). It is not surprising as wider confidence intervals are a reflection of a limited sample size. An unbiased  
577 sample is not representative of the whole population, and therefore, it is prudent that all available samples are used to fit the  
578 fragility functions.



579

580 **Fig. 11.** Fragility functions developed for manufacturing industry in (a) North Tohoku, (b) South Tohoku as well as food  
 581 industry in (c) North Tohoku and (d) South Tohoku. To evaluate the effects of preceding earthquake damage on overall damage  
 582 assessment, datasets for each industry were divided into North and South regions. Mean accuracies for each dataset were  
 583 derived using a 10-fold cross-validation to determine if the accuracies of the fragility models are affected by the compound  
 584 effect of earthquake and tsunami.

## 585 9. Conclusions

### 586 9.1 Main findings and limitations

587 We presented a first attempt to quantifying structural vulnerability of port industries to tsunami impacts by developing a  
 588 damage database for port structures and constructing damage fragility functions for various port industries. We were able to  
 589 collect damage data for more than 5000 port structures and produce damage fragility functions for eight main port industries.  
 590 Through the interpretations of our damage assessment and statistical analyses of our fragility model, a number of significant  
 591 findings have emerged from this study:

- 592 1. Energy-related and warehousing and distribution industries showed relatively higher resistance to tsunami loads,  
593 whereas chemical, cargo handling and construction materials industry appeared to be more vulnerable.
- 594 2. Using our proposed damage classification scheme, our fragility models were able to reproduce damage with  
595 prediction accuracies of up to 75%, which outperforms models created using aggregated building damage data from  
596 MLIT (Leelawat et al., 2014).
- 597 3. Pre-tsunami earthquake activities have an influence on port structural damage. It is unavoidable that the compound  
598 effects of ground shaking and liquefaction are captured in the damage data, and unaccounted for in the process of  
599 developing fragility functions. However, ground shaking appears to influence building damage at lower damage  
600 states.

601 We are also aware of other limitations of this study. One of the limitations which has repeatedly surfaced in our findings is  
602 that inundation depth alone is not sufficient to explain the damage observed in port industries. Key threshold depths were  
603 difficult to capture for all industries which suggests that by only using inundation depth as a predictor, the fragility models  
604 may underestimate the levels of damage sustained by port structures. The models can be further refined by considering other  
605 measures of damage such as other tsunami flow characteristics (e.g. velocity, hydrodynamic force), debris impacts or the  
606 effects of shielding.

## 607 **9.2 Future use of damage database and recommendations**

608 This study presents an array of potential applications in future port damage studies. First and foremost, a new damage  
609 classification scheme was proposed to characterise damage to port structures. This scheme is transferable to other study sites  
610 for damage assessment and can be applied to damage assessments through ground survey, photographic interpretation, remote  
611 sensing and machine learning techniques. Secondly, we outlined a reproducible method for damage assessment in place of an  
612 actual ground survey, especially since this assessment was performed years after the event. The manual assessment allowed  
613 us to capture damage details from a side-profile, which otherwise would have been missing from automated techniques such  
614 as change detection in remote sensing imagery. In addition, the damage database can also be used in future work to investigate  
615 the influence of different parameters such as tsunami flow characteristics, construction characteristics and etcetera on the  
616 damage observed. Last but not least, our findings, quantified through the development of fragility functions, can be used to  
617 estimate damage to port structures in future tsunami events. They can also be used to motivate improvement in structural  
618 designs, tsunami mitigation measures as well as current methods of damage assessment. However, caution must be exercised  
619 when applying these models outside of Japan as structural integrity differs from place to place, though we expect that there  
620 would be less regional variability for port industries as compared to building codes in houses and commercial buildings.  
621 We invite and provide recommendations for potential users to expand the database and improve the predictive ability of the  
622 existing fragility models:

- 623 1. Expand the database by collecting damage data from other events and improve the quality of the database by providing  
624 more details on the (i) origin of tsunami, (ii) coastal morphological setting, and (iii) method of data collection.

- 625 2. Perform tsunami simulation to collect other intensity measures such as velocity and hydrodynamic force.
- 626 3. Study the performance of buildings and port infrastructure separately. This would, however, require a larger dataset
- 627 than presented in this study because fragility models built on smaller sample sizes tend to have greater uncertainty.
- 628



629 **Data availability**

630 The database provides a comprehensive inventory of port structures and their associated damage in the 2011 Great East Japan  
631 tsunami. The database is available through an unrestricted data repository (DR-NTU) hosted by Nanyang Technological  
632 University (<https://doi.org/10.21979/N9/OTZMT1>) (Chua et al., 2020). A database guide is provided in the supplementary.

633

634 **Author contribution**

635 CTC designed the study, collected all data and information, performed all statistical analysis and prepared the manuscript.  
636 ADS provided direction for conceptualisation and advice on paper structure. AS provided the original MLIT damage data and  
637 provided guidance on the development of fragility functions. LL and KP provided advice on structural response and tsunami  
638 behaviour. DL provided advice for statistical analysis and development of fragility functions. IC provided advice on building  
639 damage assessment and development of damage database. TC provided advice for statistical analysis and developed code for  
640 bootstrapping techniques. AC assisted in the development of the damage database. SJ and NW provided general direction of  
641 paper. All authors contributed to the scientific discussion of the methods and results, as well as the editing of the manuscript.

642

643 **Competing interests**

644 The authors declare no competing interests.

645

646 **Acknowledgements**

647 This research was supported by the Earth Observatory of Singapore via its funding from the National Research Foundation  
648 Singapore and the Singapore Ministry of Education under the Research Centres of Excellence initiative. This work comprises  
649 EOS contribution number 329. The project was funded by SCOR Reinsurance Asia-Pacific. We are grateful for the support  
650 and advice we have received from Paul Nunn (SCOR Global P&C) and Nigel Winspear (formerly SCOR Global P&C). This  
651 work formed part of the PhD study of CTC, who received funding from the Nanyang Research Scholarship. This study was  
652 supported in part by the facilities and staff at the International Research Institute of Disaster Science (IRIDeS, Tohoku  
653 University). Special thanks go to Professor Fumihiko Imamura, the director of the International Research Institute of Disaster  
654 Science, for supporting and hosting the PhD student in IRIDeS. AS and KP were funded and supported by Tokio Marine &  
655 Nichido Fire Insurance Co., Ltd. and Willis Research Network (WRN). We would also like to thank Janneli Lea Soria, Stephen  
656 Chua and Jędrzej Majewski for providing feedback on the organisation of the manuscript.

657

658 **References**

- 659 [AIR Worldwide: AIR Construction and Occupancy Class Code, https://docs.air-worldwide.com/Validation/5.0/](https://docs.air-worldwide.com/Validation/5.0/index.htm#Exposure_Data/Industrial_Facility_Occupancies.htm)  
660 [index.htm#Exposure\\_Data/Industrial\\_Facility\\_Occupancies.htm](https://docs.air-worldwide.com/Validation/5.0/index.htm#Exposure_Data/Industrial_Facility_Occupancies.htm), last access: 05 April 2021, 2019.
- 661 Akiyama, M., Frangopol, D.M., Arai, M. and Koshimura, S.: Reliability of bridges under tsunami hazards: Emphasis on the  
662 2011 Tohoku-oki earthquake, *Earthquake Spectra*, 29, 295-314, <https://doi.org/10.1193/1.4000112>, 2013.
- 663 Ananth, C. V. and Kleinbaum, D. G.: Regression models for ordinal responses: a review of methods and applications,  
664 *International Journal of Epidemiology*, 26, 1323-1333, <http://doi.org/10.1093/ije/26.6.1323>, 1997.
- 665 Attary, N., Van De Lindt, J. W., Barbosa, A. R., Cox, D. T. and Unnikrishnan, V. U.: Performance-based tsunami engineering  
666 for risk assessment of structures subjected to multi-hazards: tsunami following earthquake, *Journal of Earthquake Engineering*,  
667 1-20 (2019).
- 668 Benazir, Syamsidik and Luthfi M.: Assessment on Damages of Harbor Complexes Due to Impacts of the 2018 Palu-Donggala  
669 Tsunami, Indonesia, in: *International Conference on Asian and Pacific Coasts*, edited by Nguyen, T. V., Dou, X. and Tran, T.  
670 T., Springer, Singapore, [https://doi.org/10.1007/978-981-15-0291-0\\_36](https://doi.org/10.1007/978-981-15-0291-0_36), 2019.
- 671 Building Centre of Japan: Introduction to Building Standard Law: Building Regulation in Japan,  
672 [https://www.bcj.or.jp/upload/international/baseline/BSLIntroduction201307\\_e.pdf](https://www.bcj.or.jp/upload/international/baseline/BSLIntroduction201307_e.pdf), last access: 15 October 2020, 2013.
- 673 Charvet, I., Ioannou, I., Rossetto, T., Suppasri, A. and Imamura, F.: Empirical fragility assessment of buildings affected by the  
674 2011 Great East Japan tsunami using improved statistical models, *Natural Hazards*, 73, 951-973,  
675 <https://doi.org/10.1007/s11069-014-1118-3>, 2014.
- 676 Charvet, I., Macabuag, J. and Rossetto, T.: Estimating tsunami-induced building damage through fragility functions: critical  
677 review and research needs, *Frontiers in Built Environment*, 3, 36, <https://doi.org/10.3389/fbuil.2017.00036>, 2017.
- 678 Charvet, I., Suppasri, A., Kimura, H., Sugawara, D. and Imamura, F.: A multivariate generalized linear tsunami fragility model  
679 for Kesennuma City based on maximum flow depths, velocities and debris impact, with evaluation of predictive accuracy,  
680 *Natural Hazards*, 79, 2073-2099, <https://doi.org/10.1007/s11069-015-1947-8>, 2015.
- 681 Chen, C., Melville, B. W., Nandasena, N. A. K., Shamseldin, A. Y. and Wotherspoon, L.: Experimental study of uplift loads  
682 due to tsunami bore impact on a wharf model, *Coastal Engineering*, 117, 126-137,  
683 <https://doi.org/10.1016/j.coastaleng.2016.08.001>, 2016.

684 Chua, C.T., Switzer, A.D., Suppasri, A., Li, L., Pakoksung, K., Lallemand, D., Jenkins, S., Charvet, I., Chua, T., Cheong, A.  
685 & Winspear, N.: Tsunami damage to ports: Cataloguing damage to create fragility functions from the 2011 Tohoku event,  
686 <https://doi.org/10.21979/N9/OTZMT1>, 2020.

687 Cruz, E. F., and Valdivia, D.: Performance of industrial facilities in the Chilean earthquake of 27 February 2010, *The Structural*  
688 *Design of Tall and Special buildings*, 20, 83-101, <https://doi.org/10.1002/tal.679>, 2011.

689 De Risi, R., Goda, K., Mori, N., and Yasuda, T.: Bayesian tsunami fragility modeling considering input data uncertainty,  
690 *Stochastic Environmental Research and Risk Assessment*, 31, 1253-1269, <https://doi.org/10.1007/s00477-016-1230-x>, 2017.

691 European Sea Ports Organisation: Trends in EU Ports Governance 2016.  
692 [https://www.espo.be/media/Trends\\_in\\_EU\\_ports\\_governance\\_2016\\_FINAL\\_VERSION.pdf](https://www.espo.be/media/Trends_in_EU_ports_governance_2016_FINAL_VERSION.pdf) last access: 23 October 2020,  
693 2016.

694 Fraser, S., Raby, A., Pomonis, A., Goda, K., Chian, S.C., Macabuag, J., Offord, M., Saito, K. and Sammonds, P.: Tsunami  
695 damage to coastal defences and buildings in the March 11th 2011 Mw 9.0 Great East Japan earthquake and tsunami, *Bulletin*  
696 *of Earthquake Engineering*, 11, 205-239, <https://doi.org/10.1007/s10518-012-9348-9>, 2013.

697 Geospatial Information Authority of Japan: Aerial photograph of the affected area.  
698 [https://www.gsi.go.jp/BOUSAI/h23\\_tohoku.html](https://www.gsi.go.jp/BOUSAI/h23_tohoku.html), last access: 23 October 2020, 2012a.

699 Geospatial Information Authority of Japan: Oblique photograph of the affected area.  
700 [https://www.gsi.go.jp/BOUSAI/h23\\_tohoku.html](https://www.gsi.go.jp/BOUSAI/h23_tohoku.html), last access: 23 October 2020, 2012b.

701 Geospatial Information Authority of Japan: Map/Aerial Photo Browsing Service. <http://mapps.gsi.go.jp/maplibSearch.do#1>,  
702 last access: 23 October 2020, 2013.

703 Gokon, H., Koshimura, S., Imai, K., Matsuoka, M., Namegaya, Y. and Nishimura, Y.: Developing fragility functions for the  
704 areas affected by the 2009 Samoa earthquake and tsunami. *Natural Hazards and Earth System Sciences*, 14, 3231,  
705 <https://doi.org/10.5194/nhess-14-3231-2014>, 2014.

706 Guisan, A. and Harrell, F. E.: Ordinal response regression models in ecology, *Journal of Vegetation Science*, 11, 617-626,  
707 <https://doi.org/10.2307/3236568>, 2000.

708 Hazarika, H., Kasama, K., Suetsugu, D., Kataoka, S., and Yasufuku, N.: Damage to geotechnical structures in waterfront areas  
709 of northern Tohoku due to the March 11, 2011 tsunami disaster, *Indian Geotechnical Journal*, 43, 137-152,  
710 <https://doi.org/10.1007/s40098-012-0021-7>, 2013.

- 711 Huang, J., and Chen, G.: Experimental modeling of wave load on a pile-supported wharf with pile breakwater, *Ocean*  
712 *Engineering*, 201, 107149, <https://doi.org/10.1016/j.oceaneng.2020.107149>, 2020.
- 713 Imai, K., Inazumi, T., Emoto, K., Horie, T., Suzuki, A., Kudo, K., Ogawa, M., Noji, M., Mizuto, K. and Sasaki, T.: Tsunami  
714 Vulnerability Criteria for Fishery Port Facilities in Japan, *Geosciences*, 9, 410, <https://doi.org/10.3390/geosciences9100410>,  
715 2019.
- 716 Janssen, H.: Study on the post-tsunami rehabilitation of fishing communities and fisheries-based livelihoods in Indonesia,  
717 International Collective in Support of Fishworkers, Banda Aceh/Jakarta, December 2005.
- 718 Japan Maritime Centre: The impact of the Great East Japan earthquake on the volume of seaborne cargo movement,  
719 [http://www.jpmac.or.jp/information/pdf/202\\_2.pdf](http://www.jpmac.or.jp/information/pdf/202_2.pdf) , last access: 20 September 2020, 2011.
- 720 Karafagka, S., Fotopoulou, S. and Pitolakis, K.: Analytical tsunami fragility curves for seaport RC buildings and steel light  
721 frame warehouses, *Soil Dynamics and Earthquake Engineering*, 112, 118-137, <https://doi.org/10.1016/j.soildyn.2018.04.037>,  
722 2018.
- 723 Kazama, M. and Noda, T.: Damage statistics (Summary of the 2011 off the Pacific Coast of Tohoku Earthquake damage),  
724 *Soils and Foundations*, 52, 780-792, <http://doi.org/10.1016/j.sandf.2012.11.003>, 2012.
- 725 Kihara, N., Niida, Y., Takabatake, D., Kaida, H., Shibayama, A. and Miyagawa, Y.: Large-scale experiments on tsunami-  
726 induced pressure on a vertical tide wall, *Coastal engineering*, 99, 46-63, <https://doi.org/10.1016/j.coastaleng.2015.02.009>,  
727 2015.
- 728 Koshimura, S., Namegaya, Y. and Yanagisawa, H.: Tsunami fragility: A new measure to identify tsunami damage, *Journal of*  
729 *Disaster Research*, 4, 479-488, <https://doi.org/10.20965/jdr.2009.p0479>, 2009.
- 730 Krausmann, E. and Cruz, A. M.: Impact of the 11 March 2011, Great East Japan earthquake and tsunami on the chemical  
731 industry, *Natural hazards*, 67, 811-828, <https://doi.org/10.1007/s11069-013-0607-0>, 2013.
- 732 [Kumagai, K.: Tsunami-induced Debris of Freight Containers due to the 2011 off the Pacific Coast of Tohoku](#)  
733 [Earthquake. Journal of Disaster FactSheets, 1-25, 2013.](#)
- 734 Lallemand, D., Kiremidjian, A., and Burton, H.: Statistical procedures for developing earthquake damage fragility curves,  
735 *Earthquake Engineering and Structural Dynamics*, 44, 1373-1389, <https://doi.org/10.1002/eqe.2522>, 2015.

- 736 Lam, J. S. L. and Lassa, J. A.: Risk assessment framework for exposure of cargo and ports to natural hazards and climate  
737 extremes. *Maritime Policy and Management*, 44, 1-15, <https://doi.org/10.1080/03088839.2016.1245877>, 2017.
- 738 Leelawat, N., Suppasri, A., Charvet, I. and Imamura, F.: Building damage from the 2011 Great East Japan tsunami: quantitative  
739 assessment of influential factors, *Natural Hazards*, 73, 449-471, <https://doi.org/10.1007/s11069-014-1081-z>, 2014.
- 740 Leelawat, N., Suppasri, A., Muraio, O. and Imamura, F.: A study on the influential factors on building damage in Sri Lanka  
741 during the 2004 Indian Ocean tsunami, *Journal of Earthquake and Tsunami*, 10, 1640001,  
742 <https://doi.org/10.1142/S1793431116400017>, 2016.
- 743 Leone, F., Lavigne, F., Paris, R., Denain, J. C. and Vinet, F.: A spatial analysis of the December 26th, 2004 tsunami-induced  
744 damages: Lessons learned for a better risk assessment integrating buildings vulnerability, *Applied Geography*, 31, 363-375,  
745 <https://doi.org/10.1016/j.apgeog.2010.07.009>, 2011.
- 746 Li, L., Switzer, A. D., Wang, Y., Chan, C. H., Qiu, Q., and Weiss, R.: A modest 0.5-m rise in sea level will double the tsunami  
747 hazard in Macau. *Science Advances*, 4, eaat1180, <https://doi.org/10.1126/sciadv.aat1180>, 2018.
- 748 Macabuag, J., Rossetto, T., Ioannou, I., Suppasri, A., Sugawara, D., Adriano, B., Imamura, F., Eames, I. and Koshimura, S.:  
749 A proposed methodology for deriving tsunami fragility functions for buildings using optimum intensity measures, *Natural*  
750 *Hazards*, 84, 1257-1285, <https://doi.org/10.1007/s11069-016-2485-8>, 2016.
- 751 [Macabuag, J., Rossetto, T., Ioannou, I., & Eames, I.: Investigation of the effect of debris-induced damage for constructing  
752 tsunami fragility curves for buildings. \*Geosciences\*, 8\(4\), 117, <https://doi.org/10.3390/geosciences8040117>, 2018.](https://doi.org/10.3390/geosciences8040117)
- 753 Maheshwari, B. K., Sharma, M. L. and Narayan, J. P.: Structural damages on the coast of Tamil Nadu due to tsunami caused  
754 by December 26, 2004 Sumatra earthquake, *ISET Journal of Earthquake Technology*, 42, 3, 2005.
- 755 Mas E, Koshimura S, Suppasri A, Matsuoka M, Matsuyama M, Yoshii T, Jimenez C, Yamazaki F, Imamura F.: Developing  
756 Tsunami fragility curves using remote sensing and survey data of the 2010 Chilean Tsunami in Dichato, *Natural Hazards and*  
757 *Earth System Sciences*, 12, 2689-2697, <https://doi.org/10.5194/nhess-12-2689-2012>, 2012.
- 758 Meneses, J. and Arduino, P.: Preliminary observations of the effects of ground failure and tsunami on the major ports of Ibaraki  
759 prefecture, *GEER Assoc. Rep. No. GEER-025c*, 2011.
- 760 Ministry of Land Infrastructure and Transportation (MLIT): Investigation of the impact on business activities due to the  
761 suspension of port functions in the Great East Japan Earthquake: Questionnaire survey results.  
762 [http://www.thr.mlit.go.jp/bumon/kisya/kisyah/images/38985\\_1.pdf](http://www.thr.mlit.go.jp/bumon/kisya/kisyah/images/38985_1.pdf), last access: 15 September 2020, 2011.

- 763 Ministry of Land Infrastructure and Transportation (MLIT): Survey of tsunami damage condition,  
764 <http://www.mlit.go.jp/toshi/toshi-hukkou-arkaibu.html>, last access: 23 October 2020, 2014.
- 765 Muhari, A., Charvet, I., Tsuyoshi, F., Suppasri, A. and Imamura, F.: Assessment of tsunami hazards in ports and their impact  
766 on marine vessels derived from tsunami models and the observed damage data, *Natural Hazards*, 78, 1309-1328,  
767 <https://doi.org/10.1007/s11069-015-1772-0>, 2015.
- 768 [Naito, C., Cercone, C., Riggs, H. R., & Cox, D.: Procedure for site assessment of the potential for tsunami debris](#)  
769 [impact. \*Journal of Waterway, Port, Coastal, and Ocean Engineering\*, 140\(2\), 223-232, 2014.](#)
- 770 Nayak, S., Reddy, M. H. O., Madhavi, R. and Dutta, S. C.: Assessing tsunami vulnerability of structures designed for seismic  
771 loading, *International Journal of Disaster Risk Reduction*, 7, 28-38, <https://doi.org/10.1016/j.ijdr.2013.12.001>, 2014.
- 772 Nistor, I., Palermo, D., Nouri, Y., Murty, T. and Saatcioglu, M.: Tsunami-induced forces on structures, in: *Handbook of coastal*  
773 *and ocean engineering*, edited by Kim, C.Y., World Scientific, Singapore, 261-286 ,  
774 [https://doi.org/10.1142/9789812819307\\_0011](https://doi.org/10.1142/9789812819307_0011), 2010.
- 775 Okazaki, T., Lignos, D. G., Midorikawa, M., Ricles, J. M., and Love, J.: Damage to steel buildings observed after the 2011  
776 Tohoku-Oki earthquake, *Earthquake Spectra*, 29, 219-243, <https://doi.org/10.1193/1.4000124>, 2013.
- 777 Otake, T., Suppasri, A. and Imamura, F.: Investigations on global tsunami risk considering port network, *JSCE Proceedings*  
778 *B2 (Coastal Engineering)*, 75, 1884-2399, [https://doi.org/10.2208/kaigan.75.I\\_1321](https://doi.org/10.2208/kaigan.75.I_1321) , 2019 [in Japanese].
- 779 Ozawa, S., Nishimura, T., Suito, H., Kobayashi, T., Tobita, M. and Imakiire, T.: Coseismic and postseismic slip of the 2011  
780 magnitude-9 Tohoku-Oki earthquake, *Nature*, 475, 373-376, <https://doi.org/10.1038/nature10227>, 2011.
- 781 Park, H., Cox, D. T. and Barbosa, A. R.: Comparison of inundation depth and momentum flux based fragilities for probabilistic  
782 tsunami damage assessment and uncertainty analysis, *Coastal Engineering*, 122, 10-26,  
783 <https://doi.org/10.1016/j.coastaleng.2017.01.008>, 2017.
- 784 Paulik, R., Gusman, A., Williams, J.H., Pratama, G.M., Lin, S.L., Prawirabhakti, A., Sulendra, K., Zachari, M.Y., Fortuna,  
785 Z.E.D., Layuk, N.B.P. and Suwarni, N.W.I.: Tsunami hazard and built environment damage observations from Palu City after  
786 the September 28 2018 Sulawesi earthquake and tsunami, *Pure and Applied Geophysics*, 176, 3305-3321,  
787 <https://doi.org/10.1007/s00024-019-02254-9>, 2019.

- 788 Percher, M. Bruin, W., Dickenson, S. and Eskijian, M.: Performance of port and harbor structures impacted by the March 11,  
789 2011 Great Tohoku Earthquake and Tsunami, in: Ports 2013: Success Through Diversification, 610-619,  
790 <http://doi/10.1061/9780784413067.063>, 2013.
- 791 Pitilakis, K., Crowley, H. and Kaynia, A. M.: Introduction, in: SYNER-G: Typology Definition and Fragility Functions for  
792 Physical Elements at Seismic Risk, 1-28, Springer, Dordrecht, <http://doi.org/10.1007/978-94-007-7872-6>, 2014.
- 793 R Core Team: R: A language and environment for statistical computing, R Foundation for Statistical Computing, Vienna,  
794 Austria. <https://www.R-project.org/>, 2020.
- 795 [Reese S., Cousins W.J., Power W.L., Palmer N.G., Tejakusuma I.G., Nugrahadi S.: Tsunami Vulnerability of buildings and](#)  
796 [people in South Java—field observations after the July 2006 Java tsunami. Natural Hazards and Earth System Sciences, 7,](#)  
797 [573–589, https://doi.org/10.5194/nhess-7-573-2007, 2007.](#)
- 798 Reese, S., Bradley, B.A., Bind, J., Smart, G., Power, W. and Sturman, J.: Empirical building fragilities from observed damage  
799 in the 2009 South Pacific tsunami, Earth-Science Reviews, 107, 156-173, <https://doi.org/10.1016/j.earscirev.2011.01.009>,  
800 2011.
- 801 Rossetto, T., Ioannou, I., Grant, D. N. and Maqsood, T.: Guidelines for empirical vulnerability assessment, in: GEM technical  
802 report, GEM Foundation, Pavia, 2014.
- 803 Scawthorn, C., Ono, Y., Iemura, H., Ridha, M. and Purwanto, B.: Performance of lifelines in Banda Aceh, Indonesia, during  
804 the December 2004 Great Sumatra earthquake and tsunami. Earthquake Spectra, 22, 511-544,  
805 <https://doi.org/10.1193/1.2206807>, 2006.
- 806 Shoji, G. and Nakamura, T.: Damage assessment of road bridges subjected to the 2011 Tohoku Pacific earthquake tsunami,  
807 Journal of Disaster Research, 12, 79-89, <https://doi.org/10.20965/jdr.2017.p00792>, 2017.
- 808 Song, J., De Risi, R. and Goda, K.: Influence of flow velocity on tsunami loss estimation, Geosciences, 7, 114,  
809 <https://doi.org/10.3390/geosciences7040114>, 2017.
- 810 Sugano, T., Nozu, A., Kohama, E., Shimosako, K. I. and Kikuchi, Y.: Damage to coastal structures, Soils and Foundations,  
811 54, 883-901, <https://doi.org/10.1016/j.sandf.2014.06.018>, 2014.
- 812 Suppasri, A., Charvet, I., Imai, K. and Imamura, F.: Fragility curves based on data from the 2011 Tohoku-Oki Tsunami in  
813 Ishinomaki city, with discussion of parameters influencing building damage, Earthquake Spectra, 31, 841-868,  
814 <https://doi.org/10.1193/053013EQS138M>, 2015.

815 Suppasri, A., Mas, E., Charvet, I., Gunasekera, R., Imai, K., Fukutani, Y., Abe, Y. and Imamura, F.: Building damage  
816 characteristics based on surveyed data and fragility curves of the 2011 Great East Japan tsunami, *Natural Hazards*, 66, 319-  
817 341, <https://doi.org/10.1007/s11069-012-0487-8>, 2013.

818 Suppasri, A., Pakoksung, K., Charvet, I., Chua, C. T., Takahashi, N., Ornthammarath, T., Latcharote, P., Leelawat, N., and  
819 Imamura, F.: Load-resistance analysis: an alternative approach to tsunami damage assessment applied to the 2011 Great East  
820 Japan tsunami, *Natural Hazards and Earth System Sciences*, 19, 1807–1822, <https://doi.org/10.5194/nhess-19-1807-2019>,  
821 2019.

822 Takano, T.: Overview of the 2011 East Japan earthquake and tsunami disaster, 2011.

823 Tarbotton, C., Dall'Osso, F., Dominey-Howes, D., and Goff, J.: The use of empirical vulnerability functions to assess the  
824 response of buildings to tsunami impact: comparative review and summary of best practice, *Earth-science reviews*, 142, 120-  
825 134, <https://doi.org/10.1016/j.earscirev.2015.01.002>, 2015.

826 Technical Council on Lifeline Earthquake Engineering: Ports, in: *Tohoku, Japan, Earthquake and Tsunami of 2011: Lifeline*  
827 *Performance*, edited by Tang, A.K., American Society of Civil Engineers, 547-558,  
828 <https://doi.org/10.1061/9780784479834.ch07>, 2013.

829 The 2011 Tohoku Earthquake Tsunami Joint Survey Group.: The 2011 off the Pacific coast of Tohoku earthquake tsunami  
830 information—field survey results, Coastal Engineering Committee of the Japan Society of Civil Engineers,  
831 <https://coastal.jp/tsunami2011/> (2011).

832 Tsuji, Y., Satake, K., Ishibe, T., Harada, T., Nishiyama, A. and Kusumoto, S.: Tsunami heights along the pacific coast of  
833 northern Honshu recorded from the 2011 Tohoku and previous great earthquakes, *Pure and Applied Geophysics*, 171, 3183-  
834 3215, <https://doi.org/10.1007/s00024-014-0779-x>, 2014.

835 United States Geological Survey: M 9.1 - 2011 Great Tohoku Earthquake, Japan.  
836 [https://earthquake.usgs.gov/earthquakes/eventpage/official20110311054624120\\_30/shakemap/intensity](https://earthquake.usgs.gov/earthquakes/eventpage/official20110311054624120_30/shakemap/intensity) , last access: 16  
837 October 2020, 2020.

838 Williams, J.H., Wilson, T.M., Horspool, N., Paulik, R., Wotherspoon, L., Lane, E.M. and Hughes, M.W.: Assessing  
839 transportation vulnerability to tsunamis: Utilising post-event field data from the 2011 Tōhoku tsunami, Japan, and the 2015  
840 Illapel tsunami, Chile, *Natural Hazards and Earth System Sciences*, 20, 451–470, <https://doi.org/10.5194/nhess-20-451-2020>,  
841 2020.



842 Yung, Y. F., and Bentler, P. M.: Bootstrapping techniques in analysis of mean and covariance structures, *Advanced structural*  
843 *equation modeling: Issues and techniques*, 195-226, 1996.